

**Selective Sequential Extraction Analysis of Uranium in
Great Miami Aquifer Sediment Samples, Fernald DOE site,
Ohio**

Submitted by:

Sandia National Laboratories
Carlsbad, NM 88220

Contributing Authors:

Charles R. Bryan¹, S. Andrew Du Frane², Deborah Moir³, Cheryl Schloesslin³, and Kelsey
M. Davis¹

¹Repository Performance Department, Sandia National Laboratories, Carlsbad, NM 88220

²Department of Earth and Planetary Sciences, University of New Mexico, Albuquerque,
NM 87131

³Carlsbad Environmental Monitoring & Research Center, Carlsbad, NM 88220

April 2003

Abstract

Sequential extraction analysis of sediment samples from the uranium contaminant plume in the Great Miami Aquifer, beneath the DOE Fernald site, offers insights into the partitioning of uranium in the aquifer sediments. In this procedure, uranium is leached from the sediment sample in a series of successive extractions. First, readily exchangeable uranium is released with competing cation and anion washes. Then, carbonate minerals, amorphous Fe and Mn oxy-hydroxides, organic matter, and crystalline Fe(III) oxides/oxy-hydroxides are sequentially removed from the sample. Then, clays are broken down with a strong nitric acid treatment. Finally, the residual minerals, primarily silicates, are digested and analyzed. This procedure yields information on how the uranium is partitioned between the minerals in the aquifer sediments and allows one to evaluate the mobility of the uranium—what fraction of the whole is labile, and what fraction is sequestered in mineral structures or by mineral overgrowth and encapsulation.

The aquifer sediment samples that were analyzed came from four boreholes, vertically intersecting the groundwater contaminant plume. Whole-rock uranium concentrations in the shallow, uncontaminated samples averaged 1.4 ppm, the background concentration. Samples from the contaminant plume had higher U concentrations, with a maximum of 5.9 ppm U. Readily exchangeable uranium was released by competing ion solutions containing magnesium nitrate and sodium sulfate. It is loosely sorbed onto mineral surfaces (outer sphere), and possibly in clay interlayers, and contributes significantly to the labile fraction for contaminated sediments. In the contaminated sediments, the largest fraction of the uranium is associated with carbonate minerals. Much of this is present on the mineral surface, and is labile. However, some of the uranium associated with carbonates, perhaps as much as half, is not readily displaced and may be sequestered in the mineral structure. The amount of uranium associated with amorphous and crystalline iron oxides is minor. The fraction associated with amorphous iron oxyhydroxides appears to be sequestered, while that associated with crystalline oxyhydroxides is labile. The uranium released by the strong acid extraction step, and that remaining in the residual minerals at the end of the sequential extraction procedure, is immobile and is comparable to the amount present in the uncontaminated sediments.

Although little uranium is bound to organic material in the bulk sediment samples, fragments of wood isolated from the sediment contain high concentrations of uranium. Wood in the aquifer probably concentrates uranium through microbially-mediated reduction and precipitation; the importance of this process in sequestering uranium is difficult to evaluate, because the abundance of wood in the aquifer is unknown.

In the uncontaminated sediments, there is little labile uranium. Over half of the uranium present was released in the strong acid leach and residual mineral fractions. The largest fraction of the remainder was associated with carbonate minerals.

Duplicate analyses indicate that the greatest variability in the measured uranium fractions is in the residual mineral fraction. U-bearing accessory minerals in granitic and gneissic clasts and encapsulated in silicate minerals may account for the variability in this fraction.

1. Introduction

The Fernald, Ohio DOE site was the location of uranium processing facilities during the cold war and is currently undergoing remediation, which is scheduled to complete by 2006. Contaminated soils are being removed, and a uranium contaminant plume in the aquifer underlying the site is being remediated using pump-and-treat technology. The aquifer remediation project has continued for ten years, and more than 2000 pounds of uranium have been extracted from over ten billion gallons of groundwater to date. Accurately modeling the efficiency of the pump-and-treat remediation, and forecasting remediation completion, requires knowledge of how uranium is adsorbed or partitioned within the aquifer sediments. Uranium that is sorbed onto the surface of sediment components may be able to participate in sorption/desorption reactions. Uranium that is present in individual mineral grains at depths of tens of nanometers or greater is either structurally bound or was present as sorbed or coprecipitated phases that were encapsulated as the coating of the grain grew. Barring changes in pH, Eh, or water chemistry that could result in mineral dissolution, this uranium is sequestered permanently within the grain.

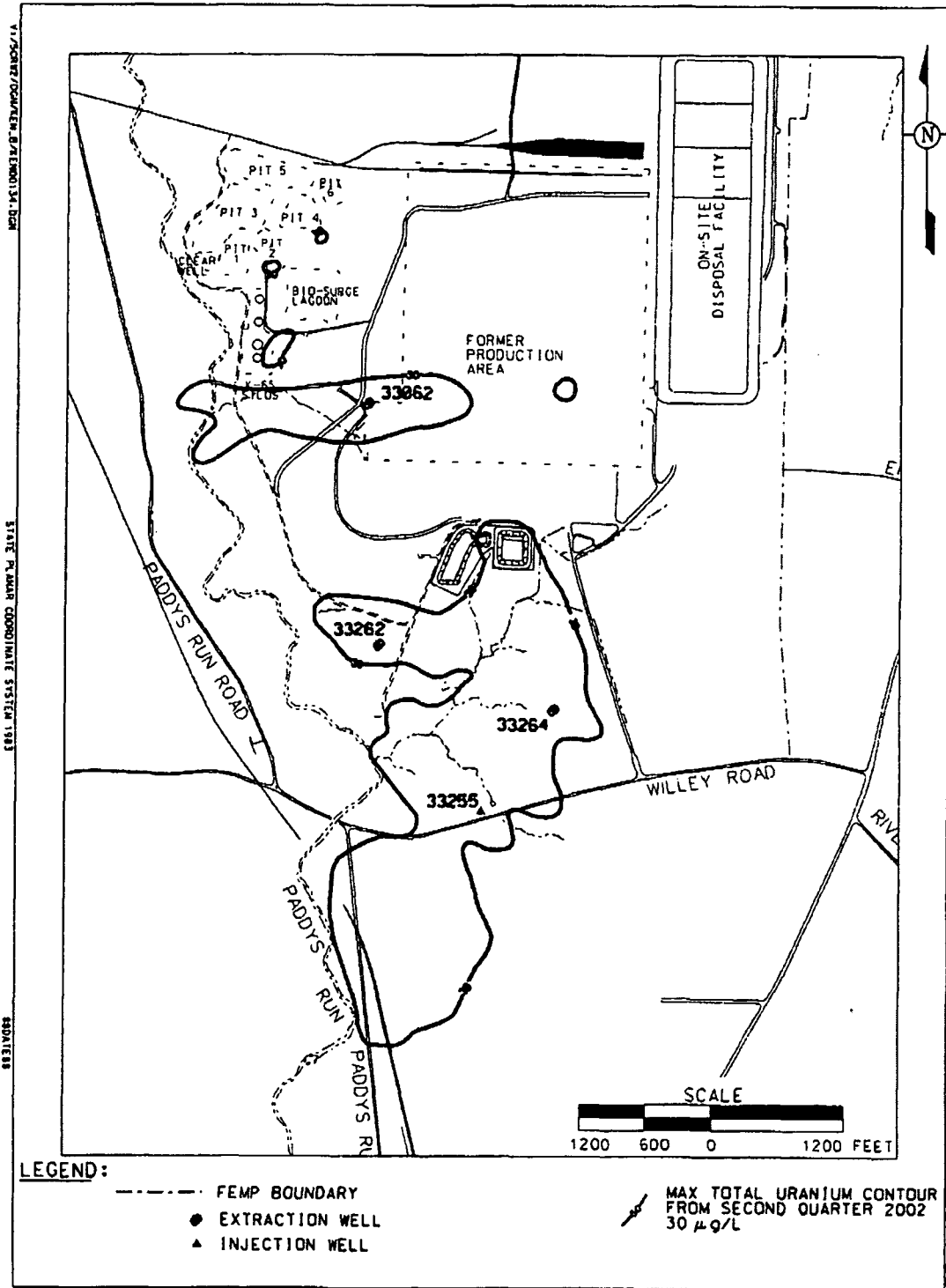
Evaluating the partitioning of uranium onto soil and sediment components is commonly accomplished through performing a set of extractions, which sequentially strip uranium fractions associated with different components out of the sample. This technique is widely used to examine the partitioning of transition metal and heavy metal contaminants in soils and sediments (see, for example Yong et al. 1993; Trolard et al. 1995; Wasay et al. 1998), and has been applied to uranium contamination by several workers (Yanase et al., 1991; Fenton and Waite, 1996; Schultz et al., 1998). Although the significance of the uranium fraction released during a sequential extraction step has been criticized as being "operationally defined," largely due to the possibility of uranium readsorption onto the remaining phases (Nirel and Morel, 1990), this technique offers valuable insights into the mobility of uranium in soils and sediments. First, the readily-exchanged uranium—that bound by ion exchange or weakly sorbed onto mineral surfaces—is extracted, and then in successive extractions, the carbonate minerals, amorphous oxyhydroxides, organic phases, and crystalline iron oxides are extracted, and the uranium released in each step is measured. The remaining residue is digested with a strong acid solution, which breaks down some clays and non-reactive oxide phases, and finally, the residue is crushed and digested with hydrofluoric acid to digest the remaining silicates and refractory phases.

The uranium fractions released in the different steps of the sequential extraction can be used to evaluate how uranium is partitioned among the mineral phases in the sediment, and to estimate the amount of mobile uranium present—that which will participate in transport, and which can be removed by pump-and-treat remediation. This parameter is necessary in order to calculate an accurate partition coefficient, or K_d , for uranium onto the aquifer sediments, and to evaluate remediation goals.

As part of this study, sediment samples were collected by Fluor-Fernald, the site manager and operator, from four areas of the aquifer: 1) the South Plume; 2) the Pilot Plant Drainage Ditch Plume; 3) aquifer sediments at the trailing edge of the South Field plume; and 4) aquifer sediments at the leading edge of the South Field plume, where U

concentrations drop abruptly, apparently due to a redox boundary see Figure 1). These samples were delivered to Sandia National Laboratories for characterization. First, all samples were analyzed for total uranium content. Then, two samples from each location were selected for further analysis. One represented the background sediments, and was collected from the sediments above the contaminant plume. The second sample was from the core of the plume. These samples were sieved into eight size fractions, and each size fraction was again analyzed for bulk uranium content. Finally, the bulk sediment samples and the finest sieve fractions ($<75 \mu\text{m}$) underwent sequential extraction analysis to characterize the uranium partitioning between the different sediment components.

All sediment characterization activities were done in the Sandia National Laboratories Carlsbad laboratory complex. Inductively-Coupled-Plasma Mass Spectrometric (ICP-MS) analysis of the whole rock digestates and sequential leachates was performed at the Carlsbad Environmental Monitoring & Research Center, a branch of New Mexico State University.



KD SAMPLE LOCATIONS

Figure 1. The location of boreholes sampled for this study.

2. Sample Descriptions

In all, 70 core samples of the Great Miami Aquifer, from four sites, were delivered to Sandia for analysis. These are summarized on Table 1. The samples were delivered in vermiculite-filled storage chests, in plastic jars with tape seals. Samples from boreholes KD33255, KD33262, and KD33264 were delivered wet, and were dried at 60 °C and sieved through an 8-mesh (2.36 mm) screen to remove rocks and pebbles. Samples from borehole KD33062A were already dried and sieved into eight size fractions (material retained in the following screens, from coarse to fine mesh: 8, 10, 20, 40, 60, 100, 200, pan) when delivered. The aquifer sediments are glaciofluvial, a mixture of silt, sand, and gravel, with relatively little clay-sized material. Detrital rock fragments and mineral grains are rounded, and consist of sedimentary carbonates and siliceous igneous and metamorphic rocks and minerals. The carbonates include dolomite and limestone (calcite); the igneous and metamorphic rock fragments include granite, monzonite(?), and granitic gneiss, containing quartz, albite, potassium feldspar, and minor ferromagnesian accessory phases. In one sample (KD33264 83.25'–84.0'), a few small (1 cm) wood fragments were recovered (these were removed from the fraction analyzed for uranium content). Samples were gray, gray-brown, or orange-brown in color, and did not visibly change color upon drying.

Table 1. Summary of samples delivered to Sandia for analysis.

Borehole #	Depth Interval, feet	# of Samples
KD33255	31 – 89	25
KD33062A	28.5 – 100.5	21
KD33262	45.2 – 67.4	12
KD33264	48.5 – 95.75	12

3. Whole-rock chemical analysis – bulk sediment samples

After drying, samples were sieved through an 8-mesh sieve to remove pebbles and gravel; the borehole 33062A samples were recombined without including the >8 mesh fraction. The samples were then split repeatedly, using a sample splitter with ½" slots, until a sample ~50 grams in size was obtained. This material was crushed using a Spex ball mill with a tungsten carbide mill to pass through a 120 mesh (125 μm) sieve. The samples were then digested and analyzed for major elements and U by ICP-MS, for organic carbon by use of a UIC Inc. carbon coulometer with a furnace front end, and for ferrous iron by titration. The procedures used for whole-rock digestion, ferrous iron determination, and total organic carbon analysis are summarized in Appendix A.

Results of the whole-rock chemical analysis of the seventy samples are presented in Figure 2 and Table 2. Each borehole transects the contaminant plume, and this is reflected in the sediment uranium concentrations. Concentrations in the shallow sediments reflect the background loading—about 1.4 ppm U. The uranium concentration increases with depth from the surface, reaches a maximum in the center of each sampled interval (corresponding to the core of the plume; Abitz, pers. comm.), and then decreases with greater depth. There was no correlation between uranium and any major element component measured in the sediments. Among the major elements, Al, K, and Na are mostly present in the silicates (clays, feldspars), and positively correlate, increasing slightly with depth, suggesting that the silicate abundances must also increase with depth. Ca and Mg also covary, and decrease with depth, presumably as the relative proportion of carbonates present decreases.

Although groundwaters in the sampled area are oxidizing (Sidle and Lee, 1996), there is significant organic carbon present in all samples, varying from 0.24 to 0.97 wt %. Wood fragments up to one cm in diameter were found in one of the sediment samples examined (KD33264 83.25'–84.0'), and wood fragments were also recovered from two other boreholes from the Fernald site and delivered to Sandia (KD33265, 78.0'–78.5'; KD33298, 66.0'–66.5'). It is unlikely, however, that this is the main source of the organic carbon in the samples, as careful examination of other samples failed to reveal any wood fragments. All of the samples contain abundant detrital limestone and dolomite and some clasts of this material were observed to give off a petroliferous odor upon crushing. Thus, much of the organic carbon may be present in the sedimentary carbonates as kerogen-like or petroliferous materials.

Reduced iron, Fe(II), is also present in the samples. Ferromagnesian minerals in the igneous and metamorphic rock fragments (magnetite, biotite, amphibole) may account for most of this. However, dolomite commonly contains trace amounts of Fe(II) in the crystal structure, and this may also contribute to the total. In addition, the wood samples described above were examined by SEM and framboidal pyrite and marcasite were observed in close association with the wood (Figure 3). Locally, siderite(?) was also present, replacing the cellular structure (Figure 4). Although not observed in the wood-

free sediments examined by SEM, in some samples, pyrite and siderite may also be contributing to the ferrous iron concentration.

It is apparent from these observations that while the bulk of the aquifer in this area may be oxidizing, there are local environments within the aquifer sediments that are reducing. These include areas where wood is present in the aquifer, and may include diffusively accessed intraclast porosity within the detrital limestone and dolomite clasts.

Table 2. Results of elemental analysis of Great Miami Aquifer sediment samples.

Borehole #	Interval sampled, ft		Concentration in rock, wt. %							FeO, wt%	TOC, wt%	U, ppm
	begin	end	Al ₂ O ₃	Fe ₂ O ₃ *	MnO	MgO	CaO	Na ₂ O	K ₂ O			
kd33255	31.00	32.00	4.63	1.74	0.04	7.30	20.85	0.93	1.06	0.60	0.35	1.29
kd33255	34.00	35.00	4.65	1.58	0.05	7.25	20.91	0.96	1.19	0.58	0.33	1.44
kd33255	35.75	37.00	4.55	1.77	0.05	7.61	21.82	0.90	1.16	0.69	0.25	1.37
kd33255	37.75	39.00	4.64	1.78	0.05	7.35	20.72	0.94	1.19	0.69	0.29	1.53
kd33255	39.00	39.50	4.39	1.55	0.05	8.23	21.68	0.82	1.11	0.59	0.27	1.40
kd33255	40.00	41.25	4.37	1.57	0.04	7.80	21.30	0.84	1.08	0.60	0.36	1.55
kd33255	41.25	42.75	4.31	1.73	0.05	7.15	20.06	0.81	1.10	1.09	0.40	1.89
kd33255	42.75	43.75	3.99	2.01	0.09	7.92	23.02	0.71	0.98	0.68	0.43	1.82
kd33255	44.00	45.50	4.23	1.66	0.05	7.97	22.83	0.83	1.10	0.68	0.54	1.81
kd33255	51.50	52.50	4.37	1.79	0.08	5.76	24.68	0.77	1.13	0.71	0.43	2.27
kd33255	53.00	54.50	5.43	2.03	0.05	5.35	21.28	1.10	1.30	0.79	0.49	2.05
kd33255	55.50	56.50	5.03	1.99	0.05	5.92	21.32	0.88	1.19	0.87	0.69	2.36
kd33255	58.50	59.50	4.94	2.04	0.05	5.19	19.49	0.97	1.16	0.84	0.30	2.94
kd33255	61.50	63.00	5.10	2.05	0.05	6.22	23.19	1.03	1.29	0.78	0.40	3.54
kd33255	65.00	66.50	4.66	1.89	0.06	6.90	20.18	0.93	1.12	0.85	0.64	3.24
kd33255	67.00	69.00	4.70	1.79	0.06	6.89	20.14	1.00	1.18	0.72	0.24	3.15
kd33255	70.50	72.00	4.97	1.94	0.05	5.38	17.75	1.05	1.25	0.81	0.30	3.48
kd33255	73.00	74.50	5.14	2.23	0.06	5.28	17.96	1.02	1.26	0.62	0.29	3.57
kd33255	74.75	77.00	5.08	2.00	0.05	5.03	16.33	1.04	1.29	0.77	0.34	3.45
kd33255	77.00	78.50	5.41	2.08	0.05	5.18	18.08	1.04	1.43	0.69	0.40	3.82
kd33255	80.00	81.50	4.45	1.88	0.05	4.90	17.87	0.82	1.17	0.74	0.28	2.68
kd33255	81.50	83.25	5.29	2.01	0.05	5.38	17.88	1.05	1.34	0.80	0.35	2.95
kd33255	83.25	84.00	4.94	1.84	0.04	4.33	16.69	0.90	1.26	0.69	0.37	3.02
kd33255	85.00	86.50	4.83	1.76	0.04	4.58	17.14	0.99	1.19	0.69	0.34	2.94
kd33255	87.50	89.00	5.01	1.77	0.04	4.26	16.93	1.03	1.30	0.83	0.36	2.80
kd33062a	28.50	29.00	4.17	1.56	0.08	4.34	18.78	0.88	1.15	0.60	0.31	1.41
kd33062a	30.00	30.50	4.76	1.82	0.06	4.80	19.91	1.01	1.22	0.59	0.34	1.70
kd33062a	34.00	34.50	4.33	1.89	0.06	4.92	20.21	0.89	1.14	0.60	0.26	1.54
kd33062a	40.50	41.00	4.54	1.97	0.05	6.09	20.00	0.88	1.09	0.85	0.30	1.61
kd33062a	46.00	46.50	4.05	1.62	0.07	8.17	22.50	0.76	1.03	0.59	0.34	1.68
kd33062a	49.00	49.50	5.50	3.06	0.08	4.15	13.67	1.33	1.30	1.28	0.45	1.84
kd33062a	52.00	52.50	5.77	2.06	0.05	3.96	12.68	1.43	1.45	0.99	0.49	2.12
kd33062a	55.00	55.50	5.10	1.63	0.05	3.98	14.89	1.15	1.33	0.80	0.44	2.18
kd33062a	58.00	58.50	5.43	1.69	0.03	4.13	11.85	1.02	1.12	0.99	0.62	2.69
kd33062a	60.50	61.00	4.95	1.69	0.05	3.58	14.65	1.29	1.36	0.85	0.48	2.97
kd33062a	64.50	65.00	4.52	1.89	0.07	5.69	21.42	0.85	1.07	0.85	0.41	3.48
kd33062a	68.00	68.50	4.56	1.73	0.04	4.45	17.69	0.98	1.25	0.74	0.39	3.46
kd33062a	70.00	70.50	4.60	1.64	0.05	4.83	17.44	1.03	1.13	1.36	0.25	2.48
kd33062a	73.00	73.50	4.49	1.66	0.05	4.54	14.48	1.04	1.24	0.40	0.37	3.15
kd33062a	78.00	78.50	5.35	1.86	0.04	4.53	16.44	1.16	1.28	1.11	0.39	2.96
kd33062a	82.00	82.50	4.87	1.91	0.04	4.93	18.03	0.90	1.18	1.01	0.33	2.57
kd33062a	85.00	85.50	4.94	1.69	0.04	3.84	14.77	1.08	1.31	0.79	0.38	2.70
kd33062a	88.00	88.50	4.97	2.11	0.05	4.38	18.06	0.93	1.16	0.98	0.34	2.68
kd33062a	94.00	94.50	6.08	2.05	0.06	3.59	15.94	1.21	1.37	1.25	0.39	2.29
kd33062a	98.00	98.50	6.04	2.50	0.06	4.08	16.48	1.33	1.40	1.24	0.33	2.11
kd33062a	100.00	100.50	6.63	2.13	0.05	3.27	14.65	1.42	1.55	1.04	0.43	2.12
kd33264	48.00	49.50	4.83	1.75	0.04	7.15	20.77	0.99	1.16	0.64	0.24	1.40
kd33264	51.80	53.00	4.55	1.68	0.05	7.82	22.16	1.00	1.18	0.48	0.24	1.43
kd33264	55.40	56.40	6.44	1.87	0.03	4.89	16.17	1.27	1.66	0.59	0.66	2.54
kd33264	74.50	75.00	5.26	1.84	0.05	6.62	23.22	1.02	1.15	0.69	0.26	2.80
kd33264	75.00	77.00	5.50	1.87	0.05	5.10	18.60	1.05	1.29	0.78	0.39	2.90
kd33264	78.00	79.50	6.05	1.90	0.05	5.17	18.51	1.24	1.48	0.69	0.97	3.01
kd33264	79.50	83.25	6.30	2.01	0.05	4.64	17.15	1.15	1.56	0.99	0.72	4.00
kd33264	83.25	84.00	5.81	1.80	0.04	4.07	15.85	1.17	1.43	0.78	0.62	3.43
kd33264	85.75	86.25	5.36	2.17	0.05	4.74	16.92	1.16	1.19	0.41	0.42	3.26
kd33264	89.00	90.25	5.07	1.94	0.06	5.07	19.41	1.02	1.23	0.68	0.38	2.38
kd33264	91.25	94.75	4.39	1.77	0.06	4.44	18.75	0.96	1.09	0.88	0.41	2.73
kd33264	94.75	95.75	6.02	1.92	0.05	3.51	13.09	1.19	1.59	0.84	0.73	3.87
kd33262	45.20	46.20	4.50	2.12	0.05	6.21	21.48	0.85	1.10	0.71	0.33	1.66
kd33262	47.25	48.25	4.45	1.64	0.04	5.83	21.31	1.06	1.10	0.58	0.32	1.60
kd33262	48.25	49.50	5.36	1.71	0.04	5.51	19.58	1.16	1.20	0.61	0.39	2.93
kd33262	50.40	51.75	5.02	2.03	0.05	4.94	19.93	0.99	1.20	0.64	0.38	3.99
kd33262	52.75	53.75	5.54	1.98	0.04	4.57	17.01	0.98	1.72	0.85	0.32	5.88
kd33262	54.50	55.75	5.11	1.77	0.04	6.14	21.66	1.09	1.18	0.65	0.32	4.50
kd33262	55.80	57.10	5.66	1.85	0.04	5.55	20.83	1.31	1.31	0.54	0.30	3.99
kd33262	57.25	58.75	4.80	1.81	0.04	5.59	20.82	1.07	1.16	0.50	0.49	3.41
kd33262	60.25	61.25	5.81	1.83	0.04	6.61	21.54	1.18	1.32	0.59	0.29	2.36
kd33262	61.80	62.80	5.30	1.78	0.04	5.35	18.68	1.15	1.25	0.50	0.43	2.25
kd33262	64.25	65.25	5.55	1.73	0.04	5.60	18.64	1.18	1.28	0.47	0.33	2.40
kd33262	66.40	67.40	5.45	1.69	0.04	5.51	18.50	1.10	1.21	0.66	0.35	2.08

Average of duplicate analyses

*total Fe as Fe₂O₃

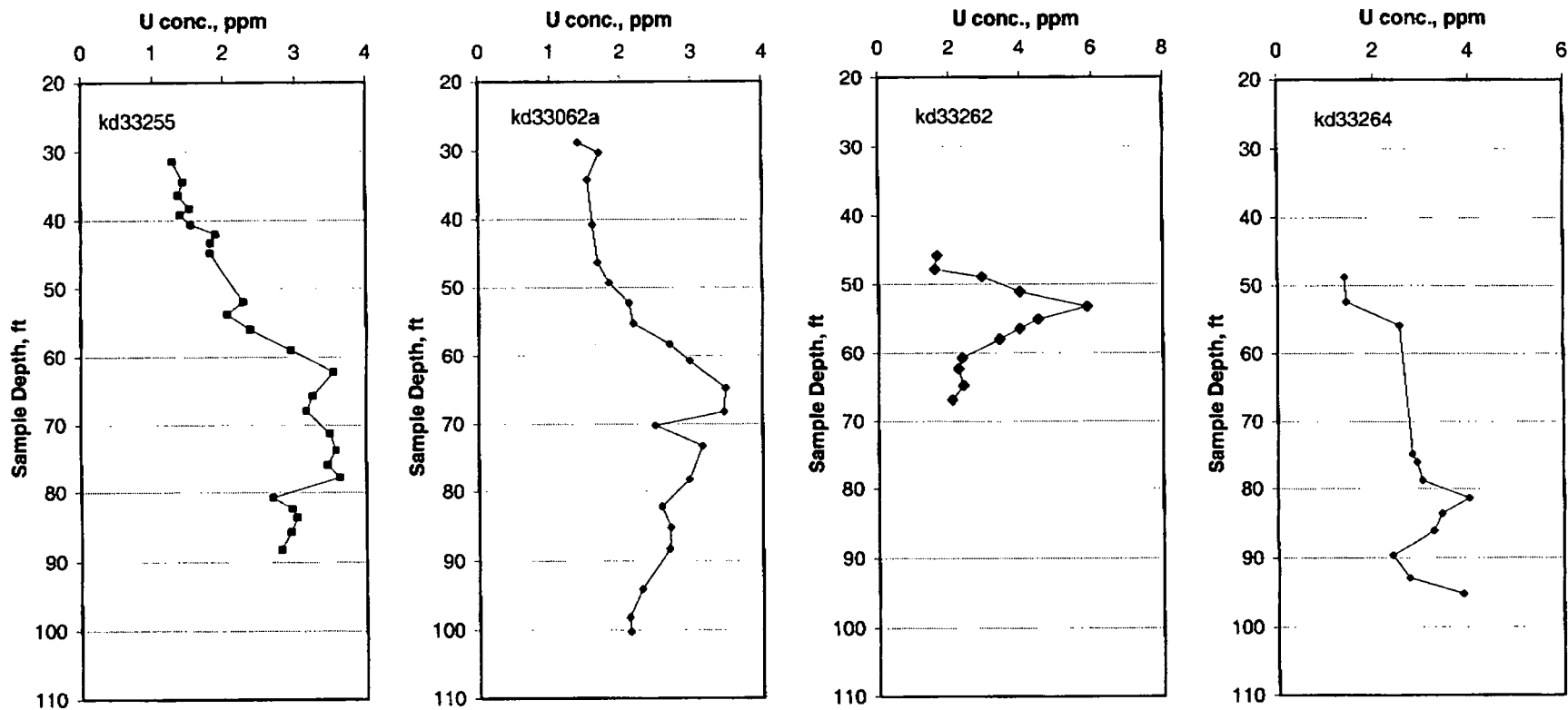


Figure 2. Uranium profile with depth, borehole sediment samples from the Great Miami Aquifer, DOE Fernald site.

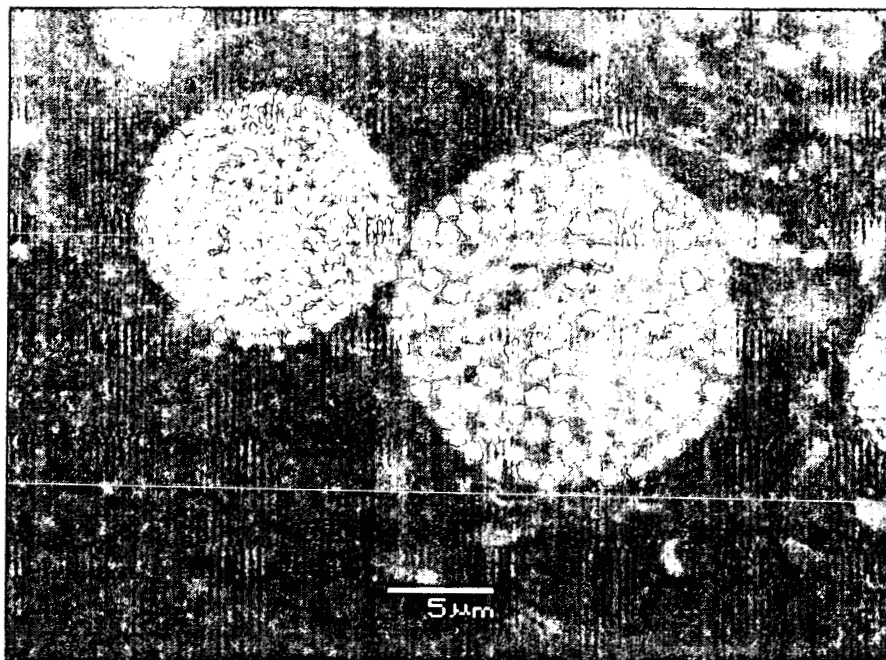


Figure 3. SEM secondary electron image of a globular cluster of pyrite octahedrons in a sample of wood recovered from borehole KD33298, at a depth of 66'–66.5'. The ordered arrangement of the pyrite octahedrons suggests that their nucleation may have been microbially-mediated.

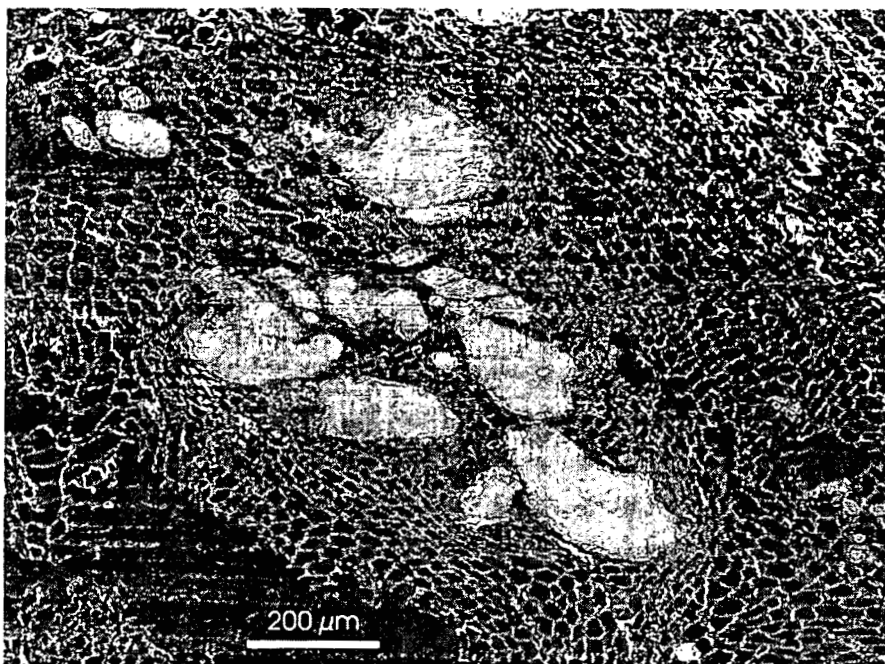


Figure 4. SEM secondary electron image of a sample of wood recovered from borehole KD33264, at a depth of 83.25'–84.0'. The cellular structure has been partially replaced with siderite (?), and the nodules of pyrite.

3. Whole-rock chemical analysis – sieve fractions of selected sediment samples

After examining the results from the whole-rock analysis, eight samples were chosen for further analysis. This set included two samples from each borehole—one from the uncontaminated part of the core (a “background” sample), and one from the most contaminated part of the core. These samples are listed in Table 3. The samples were sieved into seven size fractions, corresponding, from the largest to the smallest, to those retained in U.S. standard sieve sizes 10 (2.00 mm), 20 (850 μm), 40 (425 μm), 60 (250 μm), 100 (150 μm), 200 (75 μm), and the pan (<75 μm). After sieving, samples were split using a sample splitter with 1/2” slots to obtain a 50 gram sample for crushing and analysis. The largest size fraction, containing pebbles too coarse for the splitter, was subdivided using the pile division method to obtain a 100 gram sample for crushing.

Table 3. Sediment samples chosen for further analysis.

Sample #	Type	Sample #	Type
KD33255 34.0'–35.0'	Background	KD33262 45.2'–46.2'	Background
KD33255 73.0'–74.5'	Contaminated	KD33262 52.75'–53.75'	Contaminated
KD33062A 52.0'–52.5'	Background	KD33264 55.4'–56.4'	Background
KD33062A 64.5'–65.0'	Contaminated	KD33264 79.5'–83.25'	Contaminated

Particle size distributions for these samples are shown in Figure 5. In general, the samples consist primarily of coarse sand and pebbles, with a relatively small amount of silt and clay-sized materials. Two samples, from depths of 50-55 feet, had most abundant size fractions in the fine sand-to-silt range. There may be a relatively finer-grained sediment interlayer at this depth.

Crushed samples of each sieve fraction were digested using the method described in Appendix A, and analyzed for major elements and U by ICP-MS. The results are given in Table 4, and summarized for uranium in Figure 6. Results are similar for all the samples—U concentrations are higher in the fine fraction. This does not necessarily imply that the bulk of the uranium is in the fine fractions, however, because the mass fraction of fines is low relative to the coarser sediments. In fact, although U concentrations were highest in each case in the pan fraction, in only one of the eight samples examined did this fraction contribute the largest amount to the total uranium concentration.

In addition to chemical analyses, each sieve sample was crushed and analyzed by X-ray diffraction, using a Bruker D-8 Advance X-Ray diffractometer. The modal composition of the samples was then determined by Reitfeldt refinement, using Bruker's TOPAS-R Reitfeldt software. Only the major phases present were quantified—these were quartz, dolomite, calcite, albite, and microcline. These phases were present in all samples—one typical sample is shown in Figure 7. Diagnostic peaks for dolomite include those at 2θ angles of 31.0° (2.88Å), 41.2° (2.19Å), 50.6° (1.80Å), 51.1° (1.78Å), and 37.4° (2.40Å). Diagnostic quartz peaks are at 26.7° (3.34Å), 20.9° (4.25Å), 50.2° (1.81Å), 60.0° (1.54Å), and 36.6° (2.45Å). Quartz or dolomite is invariably the most abundant phase in the sample. Calcite is the third most abundant, with diagnostic peaks at 29.5° (3.03Å), 39.5° (2.28Å), 48.6° (1.87Å), 47.6° (1.91Å), 43.2° (2.09Å), and 23.1° (3.85Å). Albite and microcline are relatively minor phases, most of the peaks of which

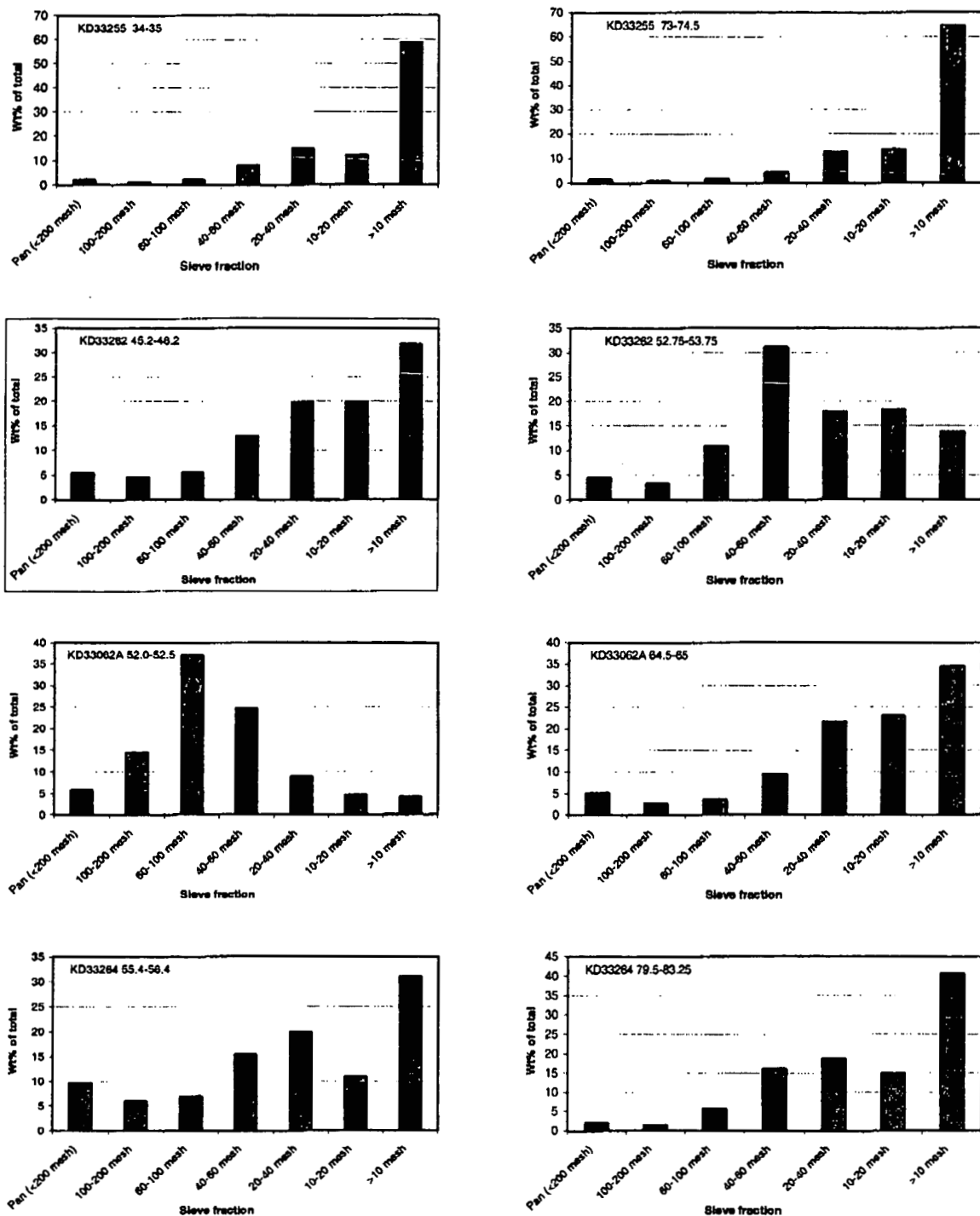


Figure 5. Particle size distributions for aquifer sediment samples from the four sampling locations. Column 1: Shallow, uncontaminated aquifer sediment samples. Column 2: Deeper sediments from the region of the groundwater contaminant plume.

Table 4. Major element and U analysis of sieve fractions from eight sediment samples.

Borehole #	Depth interval, feet	U.S. standard sieve size	Concentration in rock, wt%									U, ppm
			Al ₂ O ₃	Fe ₂ O ₃ *	MnO	MgO	CaO	Na ₂ O	K ₂ O	P ₂ O ₅		
KD33062A	52.0-52.5	Pan (<200)	4.83	2.67	0.06	6.24	20.64	0.87	1.19	0.15	4.14	
KD33062A	52.0-52.5	100-200	6.09	3.06	0.06	4.03	14.90	1.37	1.35	0.13	2.29	
KD33062A	52.0-52.5	60-100	5.57	1.65	0.04	2.60	10.43	1.34	1.38	0.08	1.73	
KD33062A	52.0-52.5	40-60	5.09	1.23	0.04	2.85	13.33	1.11	1.30	0.09	2.03	
KD33062A	52.0-52.5	20-40	4.17	1.29	0.04	3.42	17.80	0.97	1.10	0.13	2.36	
KD33062A	52.0-52.5	10-20	3.45	1.33	0.05	4.28	21.84	0.78	0.92	0.12	2.18	
KD33062A	52.0-52.5	>10	2.88	1.06	0.05	6.88	22.39	0.62	0.81	0.06	1.75	
KD33062A	64.5-65.0	Pan (<200)	4.10	2.40	0.18	8.00	23.32	0.66	1.09	0.15	9.81	
KD33062A	64.5-65.0	100-200	5.33	2.67	0.10	6.13	19.83	1.04	1.28	0.24	6.42	
KD33062A	64.5-65.0	60-100	5.66	2.47	0.08	4.20	16.67	1.19	1.29	0.18	4.39	
KD33062A	64.5-65.0	40-60	5.18	1.78	0.05	3.39	14.70	1.07	1.17	0.14	3.08	
KD33062A	64.5-65.0	20-40	4.59	1.47	0.05	4.04	18.51	1.01	1.06	0.17	2.87	
KD33062A	64.5-65.0	10-20	4.31	1.54	0.05	5.05	21.50	0.84	1.06	0.10	2.87	
KD33062A	64.5-65.0	>10	2.78	1.10	0.05	6.49	21.53	0.54	0.69	0.04	2.48	
KD33255	34.0-35.0	Pan (<200)	4.02	1.69	0.08	10.43	23.47	0.61	0.99	0.09	2.77	
KD33255	34.0-35.0	100-200	5.25	2.42	0.08	8.94	20.11	0.84	1.24	0.11	2.41	
KD33255	34.0-35.0	80-100	5.64	2.50	0.07	7.56	18.62	0.92	1.20	0.09	2.07	
KD33255	34.0-35.0	40-60	5.04	1.42	0.05	5.71	17.67	0.95	1.13	0.08	1.56	
KD33255	34.0-35.0	20-40	4.58	1.28	0.04	4.74	16.75	0.93	1.14	0.06	1.45	
KD33255	34.0-35.0	10-20	3.92	1.34	0.04	6.09	21.11	0.75	0.93	0.08	1.38	
KD33255	34.0-35.0	>10	3.14 ¹	1.09 ¹	0.03 ¹	9.72 ¹	24.82 ¹	0.76 ¹	0.67 ¹	0.04 ¹	1.35 ¹	
KD33255	73.0-74.5	Pan (<200)	4.34 ¹	2.92 ¹	0.09 ¹	9.59 ¹	23.96 ¹	0.69 ¹	1.07 ¹	0.15 ¹	10.40 ¹	
KD33255	73.0-74.5	100-200	5.52	3.44	0.08	6.80	18.73	0.87	1.24	0.15	6.68	
KD33255	73.0-74.5	80-100	6.07	2.64	0.06	4.29	15.21	1.30	1.31	0.10	4.39	
KD33255	73.0-74.5	40-60	5.38	1.85	0.04	4.33	16.03	1.07	1.20	0.09	3.86	
KD33255	73.0-74.5	20-40	4.96	1.58	0.04	4.22	17.38	0.95	1.18	0.09	3.65	
KD33255	73.0-74.5	10-20	4.69	1.68	0.04	5.06	19.66	0.88	1.09	0.09	3.46	
KD33255	73.0-74.5	>10	3.40	1.38	0.04	9.00	24.51	0.88	0.69	0.14	2.27	
KD33262	45.2-46.2	Pan (<200)	3.94	2.14	0.06	9.55	25.09	0.50	1.09	0.16	2.73	
KD33262	45.2-46.2	100-200	5.20	2.58	0.06	7.45	22.47	0.79	1.27	0.22	3.05	
KD33262	45.2-46.2	60-100	5.78	3.36	0.06	4.97	19.49	0.97	1.27	0.17	2.48	
KD33262	45.2-46.2	40-60	5.43	1.75	0.04	4.12	17.10	1.09	1.19	0.13	1.61	
KD33262	45.2-46.2	20-40	5.18	1.51	0.04	4.35	20.18	0.99	1.23	0.15	1.81	
KD33262	45.2-46.2	10-20	4.05	1.46	0.04	5.43	25.87	0.76	0.94	0.12	1.63	
KD33262	45.2-46.2	>10	1.78	0.80	0.03	11.89	29.53	0.34	0.45	0.06	1.01	
KD33262	52.75-53.75	Pan (<200)	5.12	2.53	0.04	7.49	20.81	0.53	1.34	0.16	13.69	
KD33262	52.75-53.75	100-200	6.12	3.32	0.05	5.44	18.45	0.85	1.50	0.17	9.95	
KD33262	52.75-53.75	60-100	6.49 ¹	2.12 ¹	0.04 ¹	3.72 ¹	13.20 ¹	1.24 ¹	1.51 ¹	0.11 ¹	4.91 ¹	
KD33262	52.75-53.75	40-60	5.94	1.30	0.02	2.53	10.60	1.23	1.58	0.09	4.27	
KD33262	52.75-53.75	20-40	5.40	1.45	0.03	4.21	17.91	0.96	1.40	0.11	4.49	
KD33262	52.75-53.75	10-20	4.16	1.37	0.04	4.91	24.10	0.82	0.98	0.10	4.06	
KD33262	52.75-53.75	>10	2.37	1.08	0.04	4.38	29.34	0.42	0.66	0.08	3.46	
KD33264	55.4-56.4	Pan (<200)	6.77	2.39	0.04	7.33	16.29	0.70	1.75	0.11	5.77	
KD33264	55.4-56.4	100-200	3.74	1.07	0.02	2.42	13.73	1.18	0.92	0.12	4.05	
KD33264	55.4-56.4	60-100	5.88	1.44	0.02	2.86	11.72	1.22	1.47	0.07	3.06	
KD33264	55.4-56.4	40-60	4.09	0.73	0.01	1.69	9.75	1.28	1.05	0.05	1.74	
KD33264	55.4-56.4	20-40	5.66	1.19	0.02	2.45	11.36	1.14	1.60	0.06	1.79	
KD33264	55.4-56.4	10-20	4.70	1.31	0.03	4.99	20.58	0.95	1.16	0.06	1.57	
KD33264	55.4-56.4	>10	2.25	0.86	0.03	7.74	29.19	0.47	0.49	0.04	0.98	
KD33264	79.0-82.0	Pan (<200)	5.89	2.93	0.05	8.05	16.51	0.71	1.43	0.09	9.03	
KD33264	79.0-82.0	100-200	6.70	4.08	0.07	4.98	14.49	1.06	1.53	0.12	6.52	
KD33264	79.0-82.0	60-100	6.27	1.86	0.04	3.50	12.40	1.30	1.43	0.07	3.46	
KD33264	79.0-82.0	40-60	5.01 ¹	1.18 ¹	0.03 ¹	2.65 ¹	12.06 ¹	1.31 ¹	1.26 ¹	0.06 ¹	3.44 ¹	
KD33264	79.0-82.0	20-40	5.88	1.50	0.03	3.15	12.52	1.16	1.45	0.06	3.87	
KD33264	79.0-82.0	10-20	5.00	1.60	0.05	5.43	19.12	0.85	1.22	0.07	2.98	
KD33264	79.0-82.0	>10	2.98	1.60	0.05	7.50	23.29	1.00	0.52	0.04	2.44	

¹Average of duplicate analyses

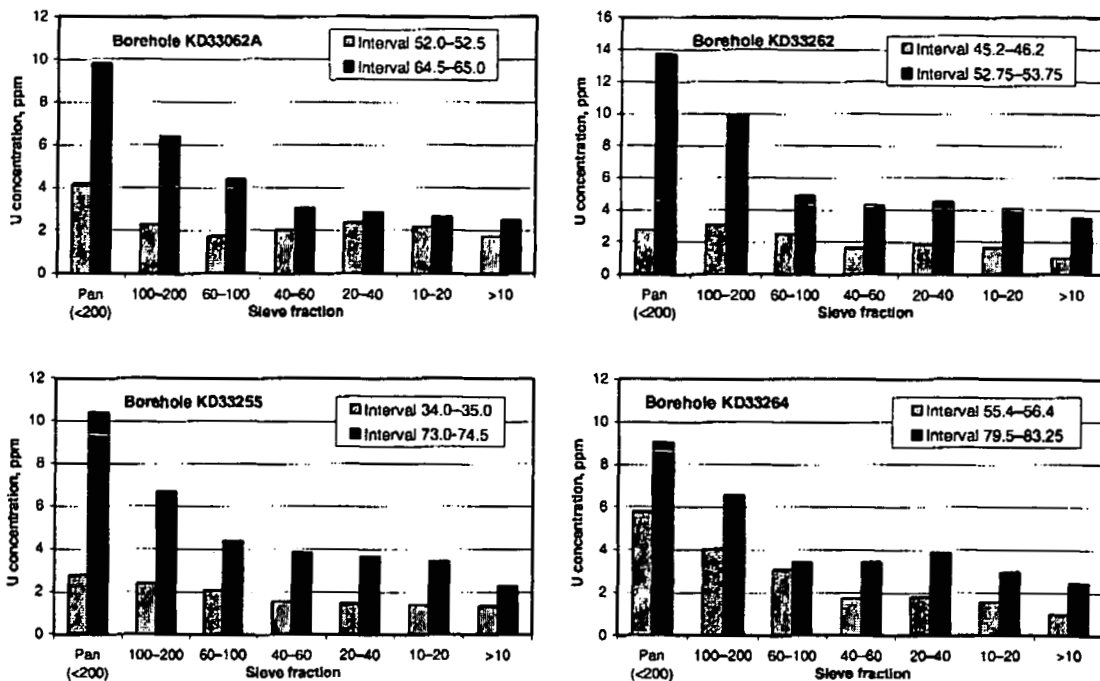


Figure 6. Concentration of uranium in different sieve fractions of borehole sediment samples. Uranium is consistently enriched in the finer fraction, and is enriched in the deeper samples, collected from the uranium contaminant plume, relative to the shallower samples from above the plume.

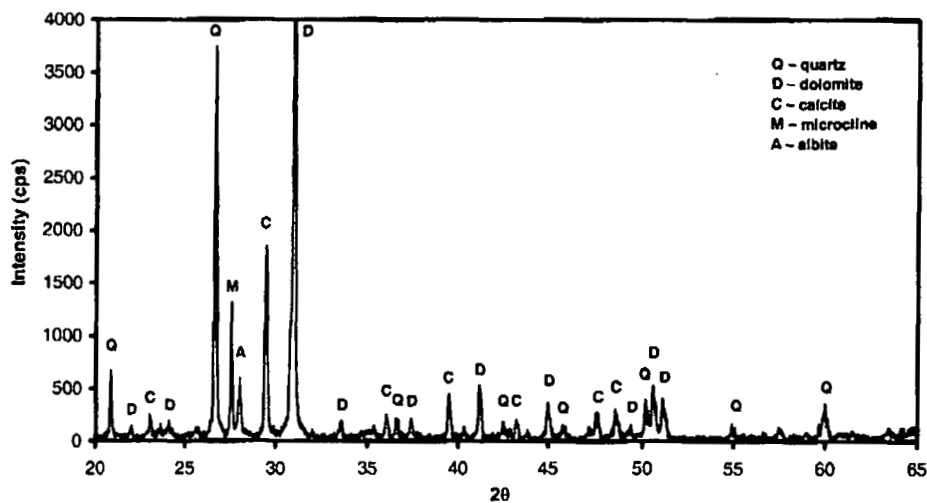


Figure 7. A typical packed powder X-ray diffraction pattern for the Great Miami Aquifer sediments examined for this study. Sample KD33262 45.2'-46.2', 100-200 mesh (75-150 μ m) sieve fraction. Major mineral peaks are labeled. The same minerals were present in all samples examined.

overlap with those of the three dominant phases. The most diagnostic peaks for albite and microcline are, respectively, at 2θ angles of 28.0° (3.18\AA) and 27.5° (3.23\AA).

The relative abundance of each phase, as determined by Rietveld analysis of the XRD spectra, is given in Table 5. Several trends are present in the data. The major silicate phases, quartz, albite, and microcline, covary, and have maximum concentrations in the intermediate sieve sizes (Figure 8). Dolomite varies inversely with the silicates, and is most abundant in the coarsest and finest size fractions. Calcite, surprisingly, does not covary with any of the other phases.

Clays constituted only a minor fraction of the bulk rock samples. Commonly, clay peaks were either not visible on the bulk rock XRD pattern or were too small to quantify. To identify the clays, the clay-sized ($<2\ \mu\text{m}$) fraction was separated from the pan (<200 mesh) size fractions of each of the eight core samples using standard settling rate techniques, and oriented clay mounts were prepared for XRD analysis (see Appendix A for details on the clay separation and mounting procedures). These mounts were then analyzed by XRD, glycolated, and reanalyzed to identify the clay minerals present. Typical XRD patterns for the air dried and glycolated clay-sized separates are shown in Figure 9. Quartz is the most intense peak in all the patterns (diagnostic peaks at 26.7° and 20.9° 2θ), and dolomite is also common (peak at 31° 2θ). Among the clay minerals, illite has the most intense peaks, at 9° , 18° , and (overlapping the quartz peak) 27° 2θ . Chlorite is also present in significant amounts, with diagnostic peaks at 12.5° , 25.1° , 6.2° , and 18.8° 2θ . Kaolinite peaks largely overlap with those of chlorite, but in most of the patterns examined, the diagnostic kaolinite peak at 24.9° 2θ can be resolved from the 25.1° chlorite peak. Glycolation has little effect upon the patterns. There is a slight decrease in the 6° chlorite peak intensities, and a broadening, or the development of a small parasitic peak, on the low angle side, indicating the presence of smectite clay.

Table 5. Modal mineral compositions of sieve fractions from Fernald sediment samples, as determined by Rietveld refinement of XRD patterns.

Sample ID	Mesh Size	Quartz	Albite	Microcline	Dolomite	Calcite
KD33255 34.0' - 35.0'	Pan (<200)	20.06	5.70	3.77	60.37	10.10
KD33255 34.0' - 35.0'	100-200	14.36	5.27	5.62	61.78	12.98
KD33255 34.0' - 35.0'	60-100	24.49	9.23	6.86	45.35	14.08
KD33255 34.0' - 35.0'	40-60	36.25	9.60	5.88	34.78	13.48
KD33255 34.0' - 35.0'	20-40	37.75	9.64	6.69	31.29	14.63
KD33255 34.0' - 35.0'	10-20	27.78	9.04	4.66	42.78	15.73
KD33255 34.0' - 35.0'	>10	13.97	5.08	2.81	68.73	9.43
KD33255 73.0' - 74.5'	>10	17.64	4.61	4.12	60.14	13.49
KD33255 73.0' - 74.5'	10-20	30.30	8.62	6.11	34.17	20.80
KD33255 73.0' - 74.5'	20-40	37.50	8.02	6.69	30.94	16.86
KD33255 73.0' - 74.5'	40-60	38.51	9.97	7.60	27.70	16.22
KD33255 73.0' - 74.5'	60-100	35.99	11.60	8.12	28.72	15.56
KD33255 73.0' - 74.5'	100-200	19.81	8.11	6.46	56.57	9.06
KD33255 73.0' - 74.5'	Pan (<200)	18.22	3.76	3.33	65.82	8.86
KD33062A 52.0' - 52.5'	>10	26.87	8.58	4.80	38.36	21.39
KD33062A 52.0' - 52.5'	10-20	18.28	11.70	7.42	28.47	36.14
KD33062A 52.0' - 52.5'	20-40	30.81	15.05	6.61	23.84	23.69
KD33062A 52.0' - 52.5'	40-60	50.22	12.24	7.94	15.11	14.49
KD33062A 52.0' - 52.5'	60-100	35.12	18.72	11.43	18.40	16.33
KD33062A 52.0' - 52.5'	100-200	33.48	18.35	5.97	27.07	15.12
KD33062A 52.0' - 52.5'	Pan (<200)	18.37	6.99	4.71	55.65	14.28
KD33062A 64.5' - 65.0'	>10	21.27	4.54	3.10	57.53	13.56
KD33062A 64.5' - 65.0'	10-20	26.34	7.30	6.39	37.53	22.44
KD33062A 64.5' - 65.0'	20-40	31.32	8.31	5.02	30.92	24.43
KD33062A 64.5' - 65.0'	40-60	43.23	10.53	6.79	21.90	17.56
KD33062A 64.5' - 65.0'	60-100	33.09	10.43	6.76	27.87	21.85
KD33062A 64.5' - 65.0'	100-200	24.97	9.77	6.59	38.00	20.67
KD33062A 64.5' - 65.0'	Pan (<200)	18.69	5.31	3.63	53.49	18.88
KD33262 45.2' - 46.2'	>10	12.75	2.41	1.83	65.78	17.22
KD33262 45.2' - 46.2'	10-20	21.12	7.78	4.42	40.23	26.45
KD33262 45.2' - 46.2'	20-40	35.65	10.38	6.12	26.34	21.50
KD33262 45.2' - 46.2'	40-60	38.72	10.40	5.33	29.00	16.55
KD33262 45.2' - 46.2'	60-100	22.44	8.80	5.31	46.69	16.77
KD33262 45.2' - 46.2'	100-200	16.47	7.42	5.82	56.73	13.56
KD33262 45.2' - 46.2'	Pan (<200)	13.34	3.92	3.84	63.17	15.73
KD33262 52.75'-53.75'	>10	18.75	3.36	2.33	42.24	33.32
KD33262 52.75'-53.75'	10-20	22.03	7.95	4.89	41.15	23.98
KD33262 52.75'-53.75'	20-40	36.52	10.41	6.87	26.89	19.31
KD33262 52.75'-53.75'	40-60	44.79	13.55	9.60	19.35	12.71
KD33262 52.75'-53.75'	60-100	41.59	12.49	7.68	24.92	13.32
KD33262 52.75'-53.75'	100-200	22.61	6.95	11.96	43.32	15.16
KD33262 52.75'-53.75'	Pan (<200)	22.07	6.54	5.78	52.86	12.76
KD33264 55.4' - 56.4'	>10	18.46	3.84	2.74	51.58	23.38
KD33264 55.4' - 56.4'	10-20	31.74	10.25	5.46	35.31	17.23
KD33264 55.4' - 56.4'	20-40	50.22	11.94	8.89	16.35	12.60
KD33264 55.4' - 56.4'	40-60	50.16	13.92	10.02	14.14	11.77
KD33264 55.4' - 56.4'	60-100	39.44	13.18	8.52	25.57	13.30
KD33264 55.4' - 56.4'	100-200	28.62	11.18	10.54	29.64	20.20
KD33264 55.4' - 56.4'	Pan (<200)	24.86	6.89	6.47	51.70	10.07
KD33264 79.5' - 83.25'	>10	24.18	5.64	2.84	52.60	14.74
KD33264 79.5' - 83.25'	10-20	30.64	7.74	4.91	37.13	19.58
KD33264 79.5' - 83.25'	20-40	45.41	11.38	8.12	20.16	14.93
KD33264 79.5' - 83.25'	40-60	45.70	12.21	8.93	20.36	12.82
KD33264 79.5' - 83.25'	60-100	42.12	14.43	9.33	19.73	14.38
KD33264 79.5' - 83.25'	100-200	30.75	10.39	8.33	39.04	11.48
KD33264 79.5' - 83.25'	Pan (<200)	33.59	7.89	6.33	41.92	10.26

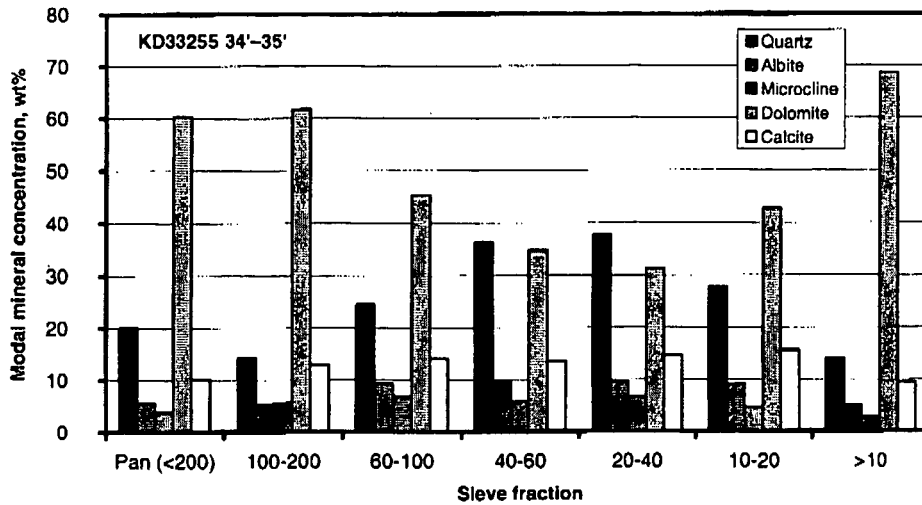


Figure 8. Plot of modal mineral abundance vs. sieve fraction for sediment sample KD33255 34'-35', illustrating the enrichment of silicates in the medium-sized particle fractions. A similar trend was observed in all of the samples examined.

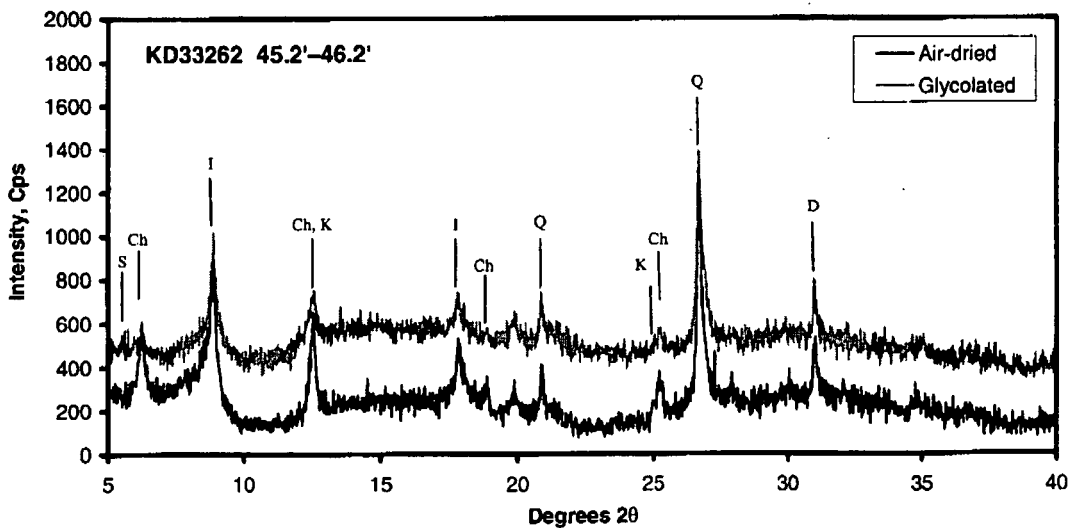


Figure 9. X-ray diffraction patterns for air-dried and glycolated clay size fractions, sample KD33262, 45.2"-46.2". Clay minerals present are illite (I), chlorite (Ch), and trace smectite (S) and kaolinite (K). All of the samples examined had similar patterns.

4. Sequential extraction analysis

After reviewing the results of the uranium analysis on the different sieve fractions, samples were chosen for sequential extraction analysis. The complete procedure is described in detail in Appendix A. The chemical extraction procedure used is the basic procedure from Tessier et al. (1979), with modifications as suggested by Chao and Zhou (1983), Rauret et al. (1989), Schultz et al. (1998), and Yanase et al. (1991)

- 1) Competing salt extraction, cations — The sediment is washed with a magnesium nitrate solution to extract uranium present as readily exchangeable cationic surface adsorbed species or ion exchangeable clay interlayer species.
- 2) Competing salt extraction, anions — The sediment was washed with a sodium sulfate solution to extract uranium present as anionic species (sulfate is a more strongly sorbing anion than the nitrate used in the first extraction step). As few common soil minerals have a positive surface charge under typical soil or aquifer conditions, anionic species are poorly sorbed, and little uranium should be released in this step.
- 3) Buffered acetic acid extraction — Carbonate minerals are digested, and uranium associated with them is released. Carbonate minerals strongly sorb uranium and commonly contain a significant fraction of the uranium present, as sorbed or encapsulated species (Yanase et al., 1991). The solution is buffered to prevent dissolution of other pH-sensitive phases (e.g., amorphous iron oxy-hydroxides).
- 4) Oxalic acid extraction — Amorphous or poorly crystalline Fe, Al, and Mn oxides/oxyhydroxides are removed by this step. Both amorphous and crystalline iron oxyhydroxides strongly sorb uranyl, and can sequester it through coprecipitation and encapsulation. Studies of natural uranium containing-soils and sediments have shown that the largest fraction of the uranium present is commonly associated with these minerals (Payne and Waite, 1991; Payne et al., 1994; Fenton and Waite, 1996; Jung et al., 1999). Ferrihydrite (amorphous iron oxyhydroxide) is of particular importance because of its high surface area, and because, when this material transforms into crystalline phases, a fraction of the sorbed uranium is not released into solution, but is permanently sequestered in the crystal structure (Payne et al. 1994, Ohnuki et al. 1997).
- 5) Peroxide extraction — This step digests organic components in the sediment. Uranyl, the expected form of U in this oxidized aquifer, complexes strongly with humic and fulvic acids (Czerwinski et al., 1994; Zeh et al., 1997), and is commonly concentrated in organic detritus in soils and sediments. In addition, such materials may be responsible for reducing microenvironments in the sediment, causing precipitation of uranium through reduction and precipitation as U(IV) species.
- 6) Dithionite extraction — This step removes crystalline ferric iron oxides/oxyhydroxides, releasing strongly sorbed, coprecipitated, or encapsulated uranium. Uranium is strongly sorbed by these phases, especially goethite (Jung et al. 1999). Uranium sorbed onto these crystalline phases will contribute to the mobile fraction. Co-precipitated or encapsulated uranium is unlikely to contribute.

- 7) Strong acid extraction — This step mostly digests clays (Yanase et al., 1991) and some refractory minerals (phosphates such as monazite and apatite, oxides). Uranium released during this step is not likely to contribute to the mobile fraction in the aquifer, and probably represents naturally occurring minerals in the sediment.
- 8) Residual solid — The remaining uranium is tied up in naturally occurring non-reactive silicates and oxides (quartz, feldspars, zircon, allanite, magnetite). Uranium sequestered in these phases will not contribute to the mobile fraction in the aquifer. This refractory residue was analyzed by hydrofluoric/nitric acid digestion.

The solutions generated in each step of the sequential extraction were analyzed for uranium and selected major elements by ICP-MS, at the Carlsbad Environmental Monitoring & Research Center.

Initially, the sequential extraction procedure was performed on bulk samples and the separated sieve fractions of two sediment samples from borehole KD33262, taken at depths of 45.2"–46.2" and 52.75"–53.75". These samples represent uncontaminated sediment from the upper part of the core containing 1.7 ppm U (Table 2), and sediment from the center of the groundwater contaminant plume, containing 5.9 ppm U (Table 2). The uranium fractions removed in each extraction are summarized in Table 6 and Figure 10; major element data are given in Appendix B (Table B-1). The bulk of the uranium in the contaminated and uncontaminated samples was removed in different steps, suggesting it is associated with different mineral phases. In the uncontaminated sample, the largest fraction of uranium—about 40%—remained in the residual, non-reactive mineral phases. An additional 15-20% was removed in the buffered acetic acid extraction and strong acid leach steps, and 5-10% in the amorphous oxide, organic, and crystalline iron oxide extractions. Only a tiny fraction of the uranium was present in a readily-exchangeable form. There is also little difference in the amounts extracted for the different sieve fractions. This indicates that the uranium is not present as sorbed species, as the surface area almost certainly varies greatly between the different sieve fractions.

The extraction results for the contaminated sample were strikingly different. The largest fraction of the uranium, about 40% of the total, was released in the buffered acetic acid extraction, in which carbonate minerals are digested. This was consistent regardless of grain size. In addition, there is much more readily-exchangeable uranium present relative to the uncontaminated sample, and this amount is dependent on the sieve fraction. In the finest sieve fraction (<200 mesh), 22% of the uranium was readily cation-exchangeable; in the coarsest (4-10 mesh), only 3%. An additional 2-6% was removed in the "anion-exchangeable" fraction, although as stated earlier, it is not clear if the uranium removed in this step is really present in an anionic form. The residual mineral fraction still contributed significantly in the contaminated sample—10-16% of the total for most size fractions. The actual amount of uranium present in the residual solids, in ng/g, is comparable to that in the uncontaminated samples, suggesting that it represents background levels. This is reasonable, as there is no clear mechanism for uranium in the contaminant plume to be sequestered in the non-reactive, highly stable minerals making up the residual mineral fraction.

Much of the uranium was extracted with the carbonate minerals. However, a significant amount of iron was also released during this extraction. This is illustrated in Figure 11 (see

Table 6. Results of sequential extractions, uncontaminated and contaminated sediment samples from borehole KD33262.

Sieve Size Fraction	Targeted uranium fraction	U removed, ng/g	
		Uncontaminated (45.2' - 46.2')	Contaminated (52.75' - 53.75')
Pan (<200 mesh)	Cation exchangeable	15	2768
	Anion exchangeable	4	515
	Carbonate minerals	239	5502
	Amorphous oxides	403	846
	Organics	189	338
	Crystalline Oxides	200	451
	Strong acid leachable	375	768
	Residual	879	1302
	Totals:	2303	12489
100-200 mesh	Cation exchangeable	—	1463
	Anion exchangeable	—	323
	Carbonate minerals	—	3360
	Amorphous oxides	—	608
	Organics	—	410
	Crystalline Oxides	—	348
	Strong acid leachable	—	886
	Residual	—	966
	Totals:		8362
60-100 mesh	Cation exchangeable	—	660
	Anion exchangeable	—	186
	Carbonate minerals	—	1930
	Amorphous oxides	—	271
	Organics	—	191
	Crystalline Oxides	—	159
	Strong acid leachable	—	570
	Residual	—	637
	Totals:		4604
40-60 mesh	Cation exchangeable	8	391
	Anion exchangeable	37	254
	Carbonate minerals	299	1585
	Amorphous oxides	82	326
	Organics	122	257
	Crystalline Oxides	77	125
	Strong acid leachable	274	277
	Residual	640	626
	Totals:	1542	3842

Table 6. Continued.

Sieve Size Fraction	Targeted uranium fraction	U removed, ng/g	
		Uncontaminated (45.2' - 46.2')	Contaminated (52.75' - 53.75')
20-40 mesh	Cation exchangeable	—	302
	Anion exchangeable	—	118
	Carbonate minerals	—	1790
	Amorphous oxides	—	480
	Organics	—	256
	Crystalline Oxides	—	191
	Strong acid leachable	—	478
	Residual	—	658
	Totals:		4271
10-20 mesh	Cation exchangeable	3	188
	Anion exchangeable	9	72
	Carbonate minerals	235	1790
	Amorphous oxides	78	507
	Organics	99	185
	Crystalline Oxides	87	281
	Strong acid leachable	242	465
	Residual	459	1238
	Totals:	1212	4726
4-10 mesh	Cation exchangeable	—	76
	Anion exchangeable	—	31
	Carbonate minerals	—	1189
	Amorphous oxides	—	218
	Organics	—	120
	Crystalline Oxides	—	155
	Strong acid leachable	—	324
	Residual	—	362
	Totals:		2474
Whole rock	Cation exchangeable	10	525
	Anion exchangeable	11	158
	Carbonate minerals	303	1879
	Amorphous oxides	117	330
	Organics	142	218
	Crystalline Oxides	118	446
	Strong acid leachable	400	272
	Residual	705	630
	Totals:	1807	4458

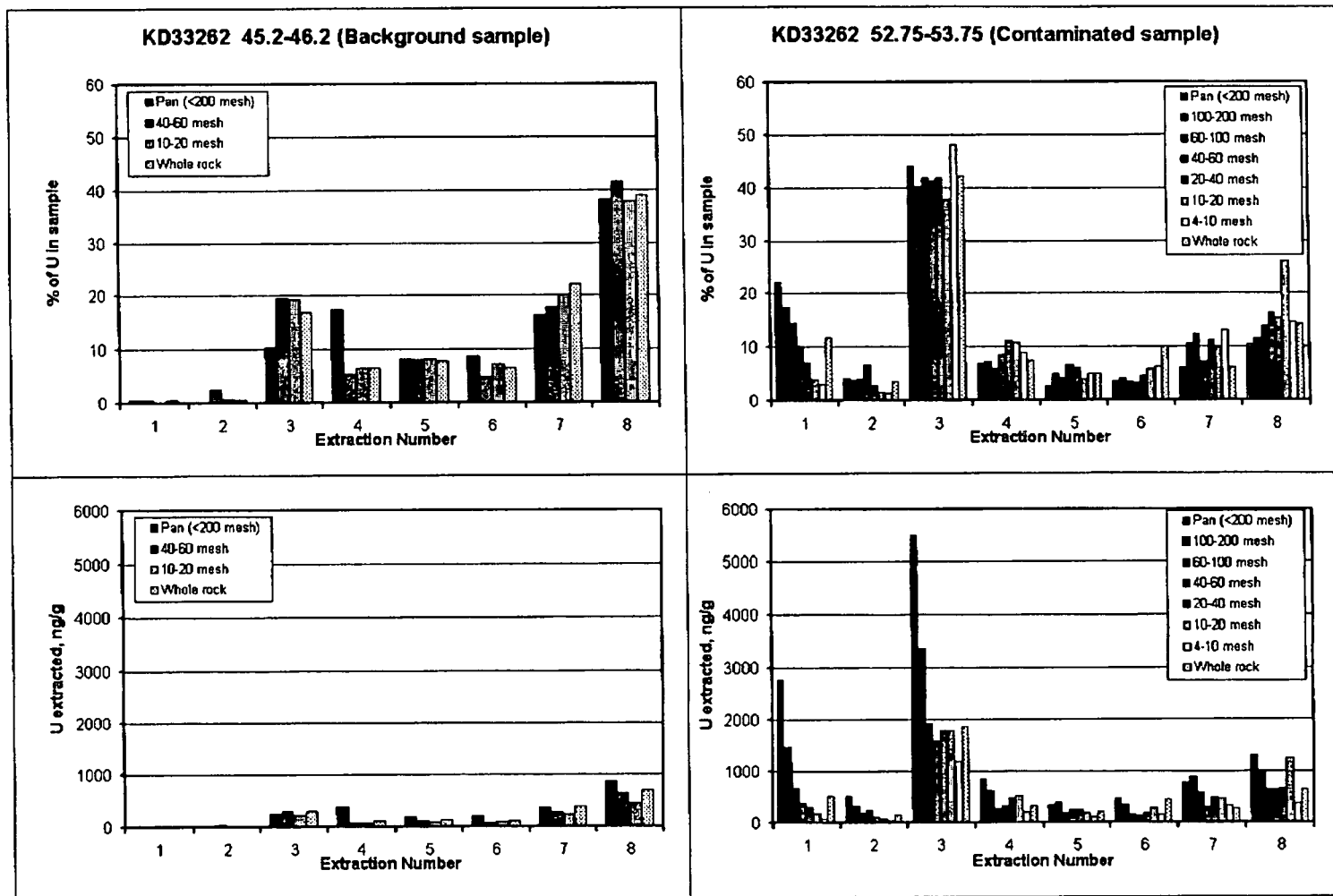


Figure 10. Fraction of uranium removed in each sequential leaching step, for different size fractions of background and contaminated samples, borehole KD33262. Top row, the percent of the total uranium removed in each step; the bottom row, the actual nanograms of uranium released per gram of sample.

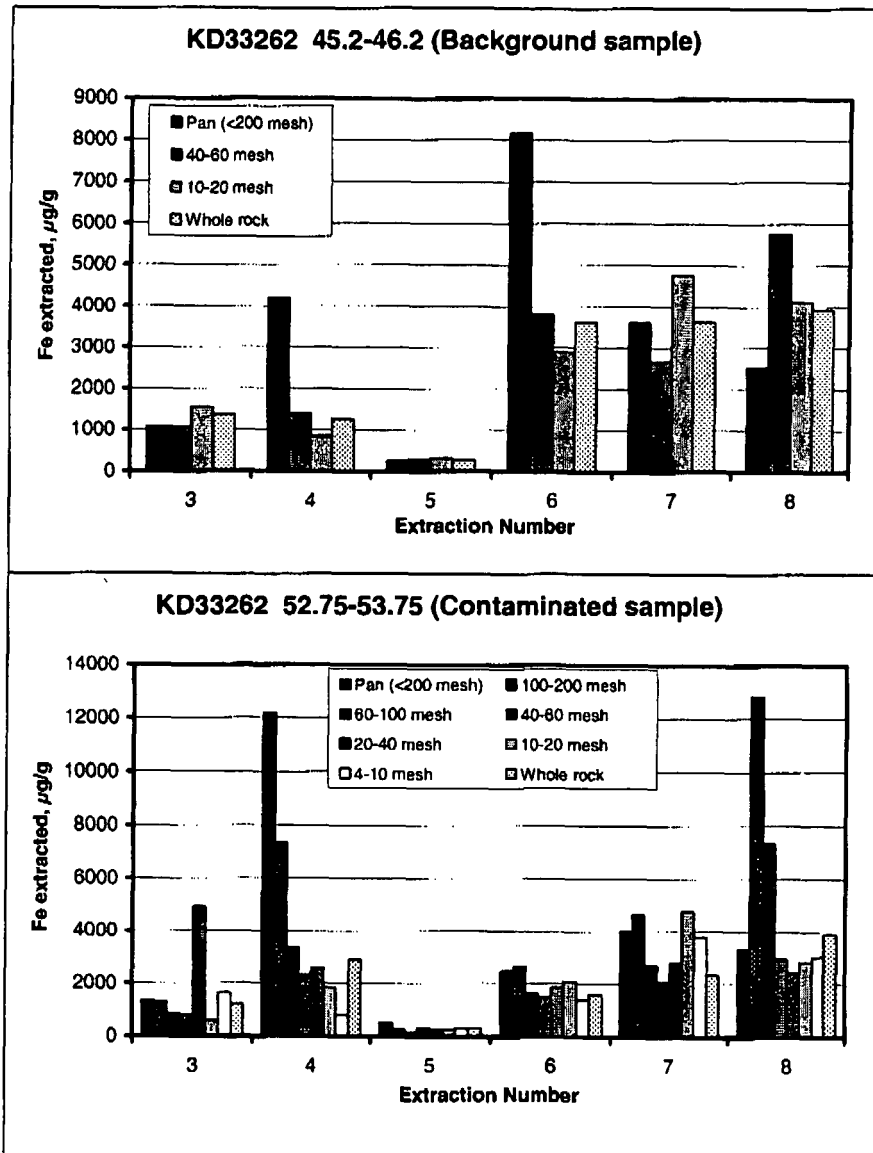


Figure 11. Iron released in sequential extraction steps 3 through 8 (Fe was not measured in steps 1 and 2). A relatively small amount of iron was released in the buffered acetic acid extraction step (3) relative to that released in the oxalic acid/ammonium acetate leach (step 4), suggesting that amorphous oxides dissolution was minor during the carbonate extraction.

Appendix B for the actual amounts of Fe removed). There is commonly a fraction of a percent of ferrous iron in the structure of dolomite—this iron would be freed during the carbonate dissolution step, and may account for the iron observed in the carbonate mineral extraction. However, Rauret et al. (1989) have shown that some fraction of the amorphous iron oxyhydroxides present can be dissolved during the buffered acetic acid extraction, especially if the extraction was of long duration. Here, the extraction was run twice, with the second extraction lasting overnight, as the dolomite dissolved only slowly—it is important to remove all carbonates, as the following steps must be carried out under acidic conditions). Thus, it is likely that some of the amorphous Fe-oxyhydroxide may have dissolved during this step.

To investigate this, the first four extractions were repeated on three of the sieve fractions from the KD33262 52-75'–53.75' sample. This time, ammonium acetate was used instead of sodium acetate, and the leachate from the first carbonate extraction step was retained and analyzed separately from the second, longer extraction. The results are shown in Table 7. For all three sieve fractions examined, slightly less uranium was extracted by the ammonium acetate extractions, but more (in one case, considerably more) iron was released. In addition, for all three samples, the ratio of uranium to iron released in the first of the two ammonium acetate treatments is considerably higher than that ratio in the second. As the second extraction was longer (lasting overnight), logically, proportionally more of the Fe and U released should have come from iron-oxides, if they were contributing to the iron content of the leachate. However, the uranium is in each case much lower in the second treatment. These data, together, suggest that the uranium released in the buffered acetic acid extraction is indeed associated with the carbonates, and not with amorphous iron oxides.

Table 7. U and Fe extracted in the carbonate mineral extraction step, using one sodium acetate extraction or two ammonium acetate extractions. Sample # KD33262 52.75'–53.75'.

Targeted uranium fraction	Sieve Size Fraction	U, ng/g extracted		Fe, µg/g extracted		
		Na-acetate	NH ₄ -acetate	Na-acetate	NH ₄ -acetate	
Cation exchangeable	Pan (<200 mesh)	2766	2595	—	—	
Anion exchangeable	Pan (<200 mesh)	515	850	—	—	
Carbonate minerals (1)	Pan (<200 mesh)	5502	3825	1346	892	1582
Carbonate minerals (2)	Pan (<200 mesh)	—	1025		—	
Amorphous oxides	Pan (<200 mesh)	846	1110	12205	11399	
Cation exchangeable	60-100 mesh	660	640	—	—	
Anion exchangeable	60-100 mesh	186	358	—	—	
Carbonate minerals (1)	60-100 mesh	1930	1210	850	647	1030
Carbonate minerals (2)	60-100 mesh	—	427		—	
Amorphous oxides	60-100 mesh	271	333	3340	3540	
Cation exchangeable	10-20 mesh	188	146	—	—	
Anion exchangeable	10-20 mesh	72	164	—	—	
Carbonate minerals (1)	10-20 mesh	1790	917	575	1012	1746
Carbonate minerals (2)	10-20 mesh	—	489		—	
Amorphous oxides	10-20 mesh	507	503	1850	1509	

Finally, sequential extractions were performed on a whole-rock sample and the pan (<200 mesh) sieve sample, in duplicate, from the contaminated zones in each of the remaining three boreholes. These samples are: KD33062A 64.5'–65.0', KD33255 73.0'–74.5', and KD33264 79.5'–83.25'. The results for uranium are shown in Table 8 and summarized in Figure 12; for the major elements, see Appendix B (Table B-2). Sample reproducibility was good—results for duplicates were very similar. Both whole rock and pan fraction samples showed similar trends in each case:

Borehole KD33062A—The largest fraction of the uranium present was released in the carbonate mineral extraction, but significant amounts were also present as exchangeable cations, and in the pan fraction, associated with the amorphous iron oxides. In the whole-rock fraction, much of the uranium was tied up in the extraction residue, and duplicate results were poor for this fraction. It is not clear why this is the case; possibly coarse detrital igneous or metamorphic mineral grains containing uranium were present.

Borehole KD33255—The largest fraction of the uranium present was released in the carbonate mineral extraction, but significant amounts were also present as exchangeable cations. In the whole-rock fraction, uranium in the extraction residue was also significant.

Borehole KD33264—Results for this sample do not match those of the others. The uranium is much more evenly distributed among the different fractions. In the fine-grained sieve sample, the combined carbonate mineral extractions account for the largest fraction of the uranium, but the extraction residue is also important. The strong acid leach, amorphous iron oxyhydroxide, and readily-exchangeable cation fractions are also significant. In the whole-rock sample, the combined carbonate extractions, the refractory mineral residue, and the strong acid leach fractions are all large. The crystalline and amorphous iron oxide fractions and the organic fraction are also significant. The smallest fractions are the exchangeable fractions.

In three of the samples, the refractory mineral residue contained a large fraction of the uranium, and reproducibility for these fractions was poor. The uranium associated with this fraction is tied up in silicates and refractory oxide minerals and will not contribute to the mobile fraction. The poor reproducibility suggests that it may be present as accessory minerals in coarse detrital igneous or metamorphic rock fragments.

Table 8. Sequential leaching results, boreholes KD33062A, KD33255, and KD33264.

Sieve Size Fraction	Targeted uranium fraction	U released, $\mu\text{g/g}$	
		Set A	Set B
KD 33062A 64.5'-65.0' Pan (<200 mesh)	Cation exchangeable	1.51	1.43
	Anion exchangeable	0.25	0.26
	Carbonate minerals	4.05	4.34
	Carbonate minerals (2)	0.93	0.83
	Amorphous oxides	0.88	0.90
	Organics	0.12	0.31
	Crystalline Oxides	0.30	0.25
	Strong acid leachable	0.35	0.36
	Residual	0.84	0.39
	Totals	9.23	9.07
KD 33062A 64.5'-65.0' Whole Rock	Cation exchangeable	0.29	0.19
	Anion exchangeable	0.10	0.08
	Carbonate minerals	0.90	0.84
	Carbonate minerals (2)	0.37	0.42
	Amorphous oxides	0.23	0.21
	Organics	0.27	0.14
	Crystalline Oxides	0.23	0.17
	Strong acid leachable	0.27	0.21
	Residual	1.08	0.55
	Totals	3.74	2.79
KD 33255 73.0'-74.5' Pan (<200 mesh)	Cation exchangeable	2.08	2.07
	Anion exchangeable	0.37	0.38
	Carbonate minerals	6.50	7.89
	Carbonate minerals (2)	0.85	0.80
	Amorphous oxides	0.82	0.80
	Organics	0.28	0.31
	Crystalline Oxides	0.26	0.20
	Strong acid leachable	0.58	0.59
	Residual	0.90	0.75
	Totals	12.6	13.8
KD 33255 73.0'-74.5' Whole Rock	Cation exchangeable	0.23	0.29
	Anion exchangeable	0.10	0.11
	Carbonate minerals	1.58	1.84
	Carbonate minerals (2)	0.36	0.61
	Amorphous oxides	0.20	0.25
	Organics	0.12	0.26
	Crystalline Oxides	0.06	0.21
	Strong acid leachable	0.22	0.31
	Residual	0.51	0.36
	Totals	3.41	4.25
KD 33264 79.5'-83.25' Pan (<200 mesh)	Cation exchangeable	0.74	0.88
	Anion exchangeable	0.41	0.35
	Carbonate minerals	1.50	1.54
	Carbonate minerals (2)	0.57	0.64
	Amorphous oxides	0.95	1.22
	Organics	0.43	0.23
	Crystalline Oxides	0.39	0.28
	Strong acid leachable	0.93	0.84
	Residual	1.32	1.70
	Totals	7.24	7.70
KD 33264 79.5'-83.25' Whole Rock	Cation exchangeable	0.13	0.16
	Anion exchangeable	0.09	0.07
	Carbonate minerals	0.41	0.44
	Carbonate minerals (2)	0.24	0.27
	Amorphous oxides	0.23	0.23
	Organics	0.36	0.24
	Crystalline Oxides	0.23	0.26
	Strong acid leachable	0.53	0.54
	Residual	0.85	0.68
	Totals	3.08	2.88

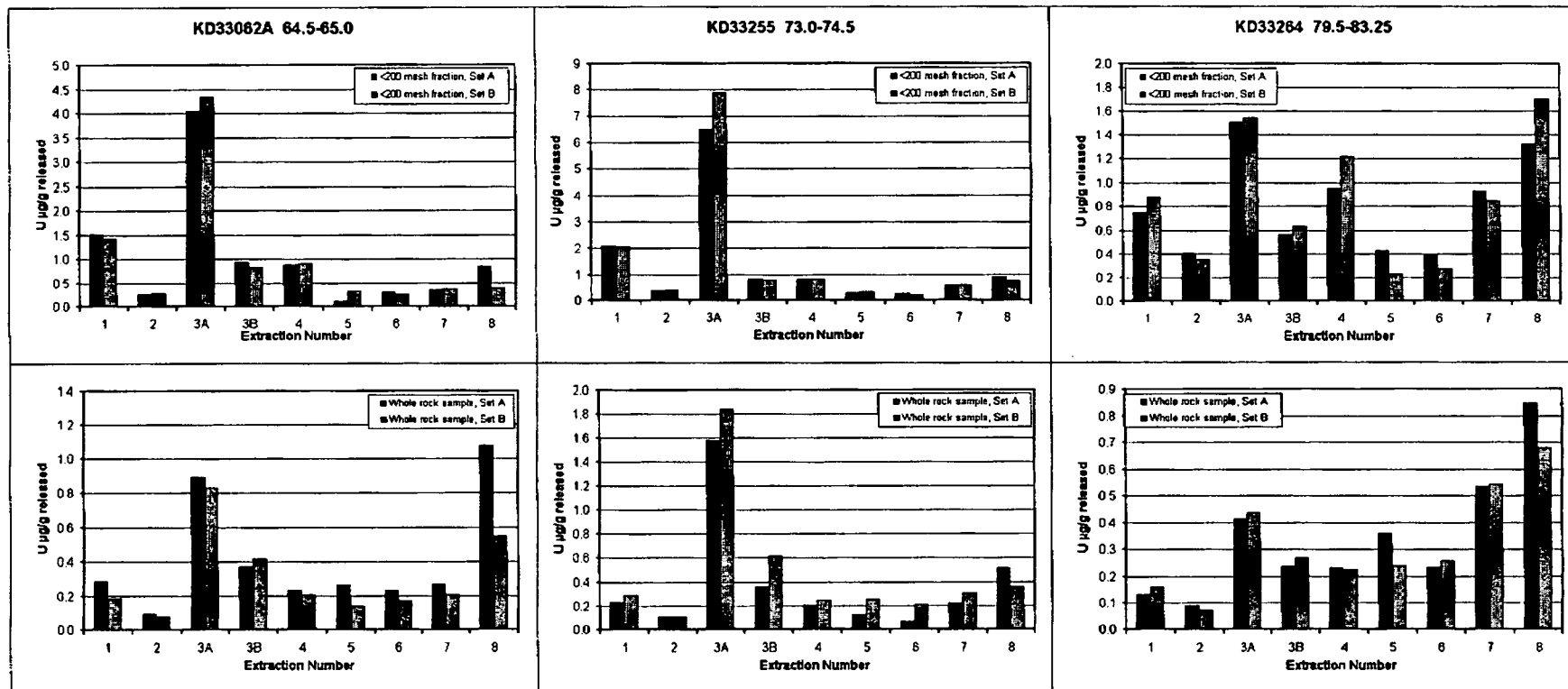


Figure 12. Sequential leaching results for whole rock samples and duplicates, from boreholes KD33062A, KD33255, and KD33264.

4. Carbonate solution leach experiments

A large fraction of the uranium in the sequential extractions was removed in the buffered acetic acid extraction, suggesting that it is associated with the carbonate minerals. However, it is also possible that the acetate, by complexing with uranium in solution, caused uranium sorbed to other phases, such as iron oxides, to desorb. Thus, the uranium in the acetic acid extraction may not represent uranium associated with carbonate minerals so much as uranium strongly sorbed onto any mineral phase. To test this, sieve fractions from one sample, KD33242 52.75'–53.75', were treated with 0.1 M sodium carbonate, and the extracted uranium was measured. Carbonate also forms strong ligand complexes with uranyl, and a concentrated solution should strip sorbed uranium off mineral surfaces. Carbonate and iron oxyhydroxide minerals are not dissolved by this treatment, so uranyl sequestered by encapsulation would not be released.

The results of the 0.1 M carbonate extractions are given in Table 9. The amount of uranium extracted from each sieve fraction decreases with increasing grain size; this is consistent with the sequential leaching results, which show that the residual and strong acid leach fractions become proportionally a larger fraction of the total U as grain size increases. The amount of uranium extracted is generally 1/3 to 2/3 of that extracted in the first six sequential extraction steps—but, these will include uranium that is encapsulated in the minerals, and is sequestered from the groundwater.

Table 9. The U fraction leached from sieve fractions of sample KD33262, 52.75'–53.75' by 0.1 M sodium carbonate.

Borehole #	Depth interval	Size Fraction	U extracted, ng/g	Total U in sample, ng/g	% of total U extracted
KD33262	52.75-53.75	Pan (<200 mesh)	6.19E+03	1.25E+04	49.6
KD33262	52.75-53.75	100-200 mesh	4.05E+03	8.36E+03	48.4
KD33262	52.75-53.75	60-100 mesh	2.13E+03	4.60E+03	46.3
KD33262	52.75-53.75	40-60 mesh	1.34E+03	3.84E+03	35.0
KD33262	52.75-53.75	20-40 mesh	1.23E+03	4.27E+03	28.8
KD33262	52.75-53.75	10-20 mesh	1.07E+03	4.73E+03	22.7
KD33262	52.75-53.75	4-10 mesh	5.19E+02	2.47E+03	21.0
KD33262	52.75-53.75	Whole rock	1.30E+03	4.46E+03	29.1

In order to better evaluate the significance of the 0.1 M carbonate extractable fraction, the pan fraction of sample KD33262, 52.75'–53.75' was treated with the 0.1 M carbonate solution, and then taken through the standard sequential extraction analysis. The results for uranium are summarized in Table 10 (see appendix B, Table B-3 for major elements). Reproducibility is good—the replicate results are very similar, and the fraction of the total uranium extracted by 0.1 M carbonate (49.6%) is the same as was measured previously (see Table 9). A comparison of the sequential extraction results for samples pretreated with 0.1 M carbonate and samples not pre-treated indicates that the uranium removed by the 0.1 M carbonate extraction consists mostly of the ion-exchangeable fraction, the fraction associated with the crystalline ferric iron

hydroxides, and about half of the fraction normally extracted into the buffered acetic acid fraction.

Table 10. Results of sequential extraction analysis of 0.1 M carbonate leached and unleached samples of the pan (<200 mesh) fraction, sample KD33262, 52.75'–53.75'.

Extraction #	Samples pretreated with 0.1 M carbonate			Samples not pretreated	
	Extracted U, ng/g		% of total avg. of 2	Extracted U, ng/g	% of total
	Rep. 1	Rep. 2			
Carb.	5570	4889	49.6	—	—
1	181	168	1.7	2766	22.1
2	102	52	0.7	515	4.1
3	2944	2925	27.9	5502	44.1
4	711	678	6.6	846	6.8
5	409	362	3.7	338	2.7
6	0	0	0.0	451	3.6
7	582	767	6.4	768	6.1
8	257	456	3.4	1302	10.4
Totals:	10756	10297	100	12489	100

5. Discussion

One of the principle goals of this study is to determine what fraction of the uranium present in the contaminated aquifer sediments is mobile, and what fraction is immobile. The immobile fraction consists of two parts. The first is that sequestered, in the crystal structures, or as encapsulated phases, in stable, low-solubility, non-reactive minerals—quartz, feldspar, and other silicates, and accessory minerals such as zircon, allanite, etc. No significant precipitation or growth of these minerals has occurred since the aquifer was contaminated, and the uranium in these minerals represents naturally occurring background. The second part of the immobile fraction consists of uranium that has been sequestered by mineral growth since the contaminant plume contacted the sediment. Minerals which may have precipitated overgrowths since exposure to the uranium plume include the carbonates and Fe, Mn, and Al oxyhydroxides (especially the amorphous ones).

It is unlikely that significant uranium mineral precipitation has occurred, as redox conditions in the contaminant plume are oxidizing, and the solubilities of most U(VI) phases have not been exceeded. However, the presence of centimeter-sized, pyrite-bearing wood fragments and measurable organic carbon in the samples indicate that locally reducing zones are present in the sediments, and uranium may be concentrated in these areas through reduction and precipitation as uraninite. Two samples of wood that were recovered from Fernald boreholes were analyzed for uranium content. The first, from borehole KD33265 78'-78.5', contained 19.6 ppm uranium. As the sample is not in the zone of the contaminant plume, this high value suggests that uranium is being concentrated in wood fragments in the aquifer sediments. Additional wood samples, from KD33298 66.0'-66.5', in the core of the contaminant plume, were supplied by Fluor-Fernald personnel. Three samples were analyzed—a bulk sample consisting of mixed sediment and wood fragments, a sample of the isolated, friable, decomposing wood fragments, and a sample of very well preserved twigs, which were partially replaced with pyrite and iron oxides. The samples had measured uranium concentrations of 21.0, 41.6, and 35.4 ppm, respectively. It is apparent that wood in the aquifer significantly concentrates uranium, probably by reduction and precipitation. This process is probably microbially mediated (Figure 2).

The relative importance of wood in sequestering uranium in the aquifer is hard to quantify, as its abundance is not known. However, wood fragments were recovered in three sediment samples from different boreholes, suggesting that it may be common enough to play an important role in fixing uranium in the aquifer.

The mobile uranium present on the aquifer sediments is that part of the total that is exchangeably bound to mineral surfaces, or in ion-exchangeable sites in mineral structures. Part of this is bound, as uranyl, into fixed-charge sites (e.g., clay interlayers), or is sorbed to mineral surfaces as outer-sphere complexes (uranium bound into the diffuse layer of the electrical double layer). Uranium bound in this manner is held by electrostatic interactions, and is easily displaced by other ions. It is released from the sample in the competing salt extractions, as the sediment is contacted with solutions containing high concentrations of Mg^{2+} and SO_4^{2-} . However, uranium bound as inner sphere complexes (that is, in the surface layer of the electrical double layer) is more strongly bound to the mineral surfaces, and is not displaced by competition with other ions.

Ideally, in the sequential extraction procedure, this fraction of the uranium is released when the mineral phase to which it is sorbed is digested.

However, there are several complicating factors. First, uranium that is released in one sequential extraction step may be readsorbed by the remaining mineral phases, and released again later, thus giving the impression that it is associated with another phase (Nirel and Morel, 1990). Also, several of the leachate solutions contain ligands (acetate, oxalate, carbonate) which complex uranyl. In high concentrations, these may strip uranium-forming inner-sphere complexes off mineral surfaces. Thus, uranium bound to iron oxides or organic materials may be removed in the buffered acetic acid wash. In addition, the extractions are only semi-selective—for instance, some of the amorphous iron oxyhydroxide will be digested in the buffered acetic acid extraction (Rauret et al. 1989).

Despite these limitations, much can be learned from the results of the sequential extraction analyses. Interpretation of the uranium fraction released in some extraction steps is unambiguous. For most of the contaminated sediments, a significant fraction of the total uranium present was released in the competing cation and anion washes. This uranium is present as uranyl in fixed-charge clay interlayer sites, and as outer-sphere sorbed species on mineral surfaces. Inner-sphere sorbed species may be released from some mineral surfaces if Mg competes effectively for the sorption sites. The uranium released in the competing cation and anion washes is clearly labile.

The largest fraction of the uranium in the contaminated samples was extracted in the buffered acetic acid wash, which extracts carbonate minerals from the sample—some amorphous iron oxyhydroxide may also be dissolved in this wash. However, when the two steps of the acetic acid extractions were analyzed separately, the bulk of the uranium was removed in the first, shorter extraction. This suggests that the uranium is associated with carbonate, rather than iron oxides. Carroll et al. (1992) examined uranyl uptake by calcite, and found that uranium-calcium solid solution is minimal, even in solutions saturated with respect to rutherfordine (UO_2CO_3). Studies by Meece and Benninger (1993), Reeder et al. (2000), and Reeder et al. (2001), also suggest that uranyl does not readily assume a stable structural environment in calcite, and long-term sequestration by calcite does not occur. Rather, uranium is sorbed as a monolayer onto the carbonate surface. Although no data are available for uranyl sorption onto dolomite, it is assumed that similar processes occur. If this is true, then the uranium extracted in the buffered acetic acid wash is likely to have been on the surface of the carbonate grains, and to be part of the labile fraction.

However, naturally-occurring calcite samples commonly have elevated uranium—rapid precipitation may favor structural incorporation of uranyl (Reeder et al. 2001). The uranium fraction released by the buffered acetic extraction was only decreased by about $\frac{1}{2}$ by the 0.1 M carbonate pretreatment, suggesting that some of the carbonate mineral-bound uranium may not be present as surface sorbed species. The proposed second half of this project, using microanalytical and spectroscopic techniques to examine the distribution of uranium in minerals and mineral coatings, may resolve this question.

In most of the contaminated samples, only a small fraction of the uranium was extracted in the oxalic acid extraction. This extraction digests amorphous Fe, Mn, and Al oxides/hydroxides,

which may have formed in the aquifer sediments either before or after the contaminant plume reached the sampling sites, or even after the sample was collected. Thus, uranium released may be sorbed onto surface of the material (characteristically, these materials have very high surface areas), or encapsulated into the material as it precipitated. Pretreating the sample with 0.1 M sodium carbonate had no effect on the magnitude of the oxalate leach fraction. Carbonate has been shown to greatly inhibit uranyl sorption to iron oxyhydroxides (Hsi and Langmuir, 1985; Morrison et al., 1995; Duff and Amrhein, 1996), and carbonate-rich solutions will leach adsorbed uranium from iron oxide minerals (Duff et al., 2002). Thus, it would appear that the uranium extracted in the oxalate leach step is not surface bound, but is sequestered by incorporation into the mineral structure as ferrihydrite was precipitated, or by encapsulation of sorbed or coprecipitated uranium phases as the mineral grew. It would follow, also, that at least part of the ferrihydrite present must postdate the contaminant plume.

The results for the dithionate extraction seem to support this conclusion. In the contaminated samples, a small fraction of uranium was released in this extraction. However, in the samples pre-treated with 0.1 M carbonate, no uranium at all was released. This suggests that virtually all of the uranium associated with the crystalline Fe(III) oxides/oxyhydroxides is surface-bound, and is part of the mobile U fraction. The sorption sites on the crystalline iron oxides are unlikely to differ from those on the amorphous materials. As the carbonate wash was effective in stripping the uranium off of the crystalline iron oxides/oxyhydroxides, but not effective in removing it from the amorphous iron oxyhydroxides, the uranium fraction associated with the amorphous oxides must be sequestered, and is not part of the mobile fraction. While ferrihydrite is easily and rapidly precipitated, recrystallization into crystalline iron oxides/oxyhydroxides is kinetically much slower. Apparently, ferrihydrite has precipitated over the time interval since the uranium plume formed, but no significant conversion to crystalline iron oxides/oxyhydroxides has occurred.

In contrast to several other studies (Payne and Waite, 1991; Payne et al., 1994; Fenton and Waite, 1996; Sato et al., 1997; Jung et al., 1999), the amorphous and crystalline iron oxides/oxyhydroxides present in the Great Miami Aquifer sediments do not appear to be the controlling phases with respect to uranium mobility. Carbonate has been shown to inhibit uranyl sorption onto goethite and ferrihydrite (Hsi and Langmuir, 1985; Morrison et al. 1995; Duff and Amrhein, 1996; Waite et al. 1996); it seems probable that reduced role of iron oxides at this site is due to the carbonate-rich (~400 $\mu\text{g/ml}$) nature of the aquifer waters.

Uranyl forms strong complexes with some organic compounds, such as humic and fulvic acids (Czerwinski et al., 1994; Zeh et al., 1997), but only a small amount of the uranium in the contaminated samples was removed in the peroxide extraction. The size of that fraction was not affected by the 0.1 M carbonate pretreatment, suggesting that this uranium is fixed. The uranium extracted in the strong acid extraction, and that remaining in the residual solids, is also immobile under aquifer conditions, and will not participate in transport.

7. Conclusions

Sequential extraction analysis of sediment samples from the uranium contaminant plume in the Great Miami Aquifer, beneath the DOE Fernald site, offers insights into the partitioning of uranium in the aquifer sediments. In the contaminated sediments, the largest fraction of the uranium is associated with carbonate mineral grains. Part of this is present on the mineral surfaces, and is labile. However, the results of the 0.1 M carbonate pretreatment suggest that some of the uranium associated with carbonates, perhaps as much as half, may be sequestered in the mineral structure. Readily exchangeable uranium was released by competing ion solutions containing magnesium nitrate and sodium sulfate. It is associated with clay minerals and loosely sorbed onto mineral surfaces, and contributes significantly to the labile fraction for contaminated sediments. The amount of uranium associated with organic materials in the bulk sediment is minor; however, wood fragments appear to significantly concentrate uranium, probably through reduction and precipitation. The importance of this process is difficult to evaluate, as the abundance of wood in the aquifer is not known. The amount of uranium associated with amorphous and crystalline iron oxides is minor. The fraction associated with amorphous iron oxyhydroxides (ferrihydrite) appears to be sequestered, while that associated with crystalline oxyhydroxides is surface-bound, and is labile. This suggests that precipitation of ferrihydrite has occurred since inception of the contaminant plume, but conversion to crystalline iron phases has been minimal. The uranium released by the strong acid extraction, and that in the residual solids, is immobile, and is comparable to the amount present in the uncontaminated sediments. In the uncontaminated sediments, there is little labile uranium; the strong acid leach and residual mineral fractions are the largest. Duplicate analyses indicate that the greatest variability in the measured uranium fractions is in the residual mineral fraction—U-bearing accessory minerals in granitic and gneissic clasts, and encapsulated in silicate minerals, may account for the variability in this fraction.

8. References

- Carroll S. A., Bruno J., Petit J. C., and Dran J. C., 1992. Interactions of U(VI), Nd and Th(IV) at the calcite-solution interface. *Radiochimica Acta*, 58/59, 245-252.
- Chao, T.T. and Zhou, L., 1983. Extraction techniques for selective dissolution of amorphous iron oxides from soils and sediments, *Soil Science Society of America Journal*, 47, 225-232.
- Czerwinski K., Buckau G., Scherbaum F., and Kim J. I., 1994. Complexation of the uranyl-ion with aquatic humic-acid. *Radiochimica Acta*, 65(2), 111-119.
- Duff, M.C., and Amrhein, C., 1996. Uranium (VI) sorption on goethite and soil in carbonate solutions, *Soil Science Society of America Journal*, 60, 1393-1400.
- Duff, M.C., Coughlin, J.U., and Hunter, D.B., 2002. Uranium co-precipitation with iron oxide minerals.
- Fenton, B.R., and Waite, T.D., 1996. A kinetic study of cation release from a mixed mineral assemblage: implications for determination of uranium uptake, *Radiochimica Acta*, 74, 251-256.
- Hsi, C. D., and Langmuir, D., 1985. Adsorption of uranyl onto ferric oxyhydroxides: application of the surface complexation site-binding model, *Geochimica et Cosmochimica Acta*, 49, 1931-1941.
- Jung, J., Hyun, S.P., Lee, J.K., Cho, Y.H., and Hahn, P.S., 1999. Adsorption of UO_2^{2+} on natural composite materials, *Journal of Radioanalytical and Nuclear Chemistry*, 242 (2), 405-412.
- Meese, D.E., and Benninge, L.K., 1993. The coprecipitation of Pu and other radionuclides with CaCO_3 , *Geochimica et Cosmochimica Acta*, 57 (7), 1447-1458.
- Morrison, S.J., Spangler, R.B., and Tripathi, V.S., 1995. Adsorption of uranium (VI) on amorphous iron oxides at high concentrations of dissolved carbon (IV) and sulfur (VI), *Journal of Contaminant Hydrology*, 17, 333-346.
- Nirel, P.M.V., and Morel, F.M.M., 1990. Pitfalls of sequential extractions, *Water Resources*, 24 (8), 1055-1056.
- Ohnuki, T., Isobe, H., Yanase, N., Nagano, T., Sakamoto, Y., and Sekine, K., 1997. Change in sorption characteristics of uranium during crystallization of amorphous iron oxides, *Journal of Nuclear Science and Technology*, 34 (12), 1153-1158.
- Payne, T.E., Davis, J.A., and Waite, T.D., 1994. Uranium retention by weathered schists – the role of iron minerals, *Radiochimica Acta*, 66/67, 297-303.
- Payne, T.E., and Waite, T.D., 1991. Surface complexation modeling of uranium sorption data obtained by isotope exchange techniques, *Radiochimica Acta*, 52/53 487-493.
- Rauret, G., Rubio, R., and Lopez-Sanchez, J.F., 1989. Optimization of Tessier procedure for metal solid speciation in river sediments, *International Journal of Environmental Analytical Chemistry*, 36, 69-83.

- Reeder, R.J., Nugent, M., Lamble, G.M., Tait, C.D., and Morris, D.E., 2000. Uranyl coprecipitation into calcite and aragonite: XAFS and luminescence studies, *Environmental Science and Technology*, 34 (4), 638-644.
- Reeder, R.J., Nugent, M., Tait, C.D., Morris, D.E., Heald, S.M., Beck, K.M., Hess, W.P., and Lanzirotti, A., 2001. Coprecipitation of uranium (VI) with calcite: XAFS, micro-XAS, and luminescence characterization, *Geochimica et Cosmochimica Acta*, 65 (20), 3491-3503.
- Sato, T., Murakami, T., Yanase, N., Isobe, H., Payne, T.E., and Airey, P.L., 1997. Iron nodules scavenging uranium in groundwater, *Environmental Science and Technology*, 31, 2854-2858.
- Schultz, M.K., Burnett, W.C., and Lin, K.G.W., 1998. Evaluation of a sequential extraction method for determining actinide fractionation in soils and sediments, *Journal of Environmental Radioactivity*, 40 (2), 155-174.
- Tessier, A., Campbell, P.G.C., and Bisson, M., 1979. Sequential extraction procedure for the speciation of particulate trace metals, *Analytical Chemistry*, 51 (7), 844-851.
- Trolard, F., Bourrie, E., Jeanroy, E., Herbillon, A.J., and Martin, H., 1995. Trace metals in natural iron oxides from laterites: a study using selective kinetic extraction, *Geochimica et Cosmochimica Acta*, 59 (7), 1285-1297.
- Yanase, N., Nightingale, T., Payne, T., and Duerden, P., 1991. Uranium distribution in mineral phases of rock by sequential extraction, *Radiochimica Acta*, 52/53, 387-393.
- Yong, R. N., Galvez-Cloutier, R., and Phadungchewit, Y., 1993. Selective sequential extraction analysis of heavy-metal retention in soil, *Canadian Geotechnical Journal*, 30, 834-847.
- Waite, T.D., Davis, J.A., Payne, T.E., Waychunas, G.A., and Xu, N., 1994. Uranium (VI) adsorption to ferrihydrite: application of a surface complexation model, *Geochimica et Cosmochimica Acta*, 58 (24), 5465-5478.
- Wasay, S.A., Barrington, S., and Tokunaga, S., 1998. Retention form of heavy metals in three polluted soils, *Journal of Soil Contamination*, 7(1), 103-119.
- Zeh P., Czerwinski K. R., and Kim J. I., 1997. Speciation of Uranium in Gorleben groundwaters. *Radiochimica Acta*, 76, (37-44).

Appendix A. Analytical Methods.

The laboratory work performed for this project was carried out under the auspices of the SNL Nuclear Waste Management Program (NWMP) Quality Assurance Program, developed to DOE specifications for work in support of the Waste Isolation Pilot Plant (WIPP). Our personnel are trained, and instruments are controlled and managed, under this extensive and rigorous QA program.

1. Whole-rock digestion procedure for U and major element analysis

Sediment samples were crushed to $<125\mu\text{m}$ (120 mesh). Approximately 0.1 g of each sample was weighed out on a calibrated analytical balance, and the weight was recorded to the nearest 0.1 mg. Each sample was transferred to a numbered Teflon Parr bomb, and 5 ml of high purity concentrated nitric acid was added. The samples were allowed to digest for five minutes to remove the carbonate (to avoid dangerous pressure build-up in the Parr bomb), and 10 ml of high purity HF was added. The Parr bombs were sealed and placed in an oven at 150 °C to digest overnight. The samples were removed from the oven, allowed to cool, and transferred quantitatively to numbered Teflon beakers—each Parr bomb was scrubbed with a rubber policeman and rinsed three times to ensure complete transfer. The samples were taken to dryness on a hot plate, leaving a white residue of fluorides in the bottom of each beaker. A few ml of high purity 1 M HCl was added, and the samples were again taken to dryness. This process was repeated two-three times, until all fluorides had been converted to chlorides, and the dissolved samples were completely clear and free of precipitate. The samples were allowed to cool, quantitatively transferred to a 25 ml volumetric flask, and brought to volume with 1 M HCl. They were then transferred to plastic bottles and stored for ICP-MS analysis. Blanks and duplicates were run to evaluate precision and reproducibility—results are summarized in Table A-1. For more detailed information, see the Carlsbad Environmental Monitoring & Research Center data package.

5635
5635

Table A-1. Results of duplicate analysis, U and major elements by ICP-MS.

Borehole #	Interval sampled, ft		Rep. #	Concentration in rock, wt%								U, ppm
	begin	end		Al ₂ O ₃	Fe ₂ O ₃ *	MnO	MgO	CaO	Na ₂ O	K ₂ O	P ₂ O ₅	
KD33255	31.0	32.0	1	4.48	1.81	0.05	7.20	20.82	0.82	1.06	0.01	1.22
			2	4.77	1.87	0.04	7.40	20.88	1.04	1.06	0.41	1.37
			Avg.	4.63	1.74	0.04	7.30	20.85	0.93	1.06	0.21	1.29
KD33255	51.5	52.5	1	4.44	1.80	0.08	5.73	24.70	0.84	1.20	0.32	2.35
			2	4.30	1.79	0.06	5.78	24.65	0.89	1.06	0.05	2.19
			Avg.	4.37	1.79	0.06	5.76	24.68	0.77	1.13	0.19	2.27
KD33255	58.5	59.5	1	5.17	2.18	0.06	5.35	20.43	0.97	1.25	0.32	2.97
			2	4.72	1.91	0.05	5.04	18.55	0.97	1.08	0.43	2.91
			Avg.	4.94	2.04	0.05	5.19	19.49	0.97	1.16	0.38	2.94
KD33255	83.25	84.0	1	4.89	1.78	0.04	4.31	16.27	0.96	1.26	0.23	3.09
			2	4.99	1.90	0.04	4.35	17.12	0.83	1.25	0.01	2.96
			Avg.	4.94	1.84	0.04	4.33	16.69	0.90	1.26	0.12	3.02
KD33062a	40.5	41.0	1	4.47	1.92	0.05	5.76	20.06	0.97	1.13	0.24	1.67
			2	4.61	2.02	0.05	6.42	19.94	0.79	1.05	0.01	1.55
			Avg.	4.54	1.97	0.05	6.09	20.00	0.88	1.09	0.13	1.61
KD33062a	64.5	65.0	1	4.51	1.83	0.07	5.49	20.31	0.96	1.05	0.26	3.50
			2	4.54	1.95	0.08	5.90	22.53	0.74	1.08	0.05	3.46
			Avg.	4.52	1.89	0.07	5.69	21.42	0.85	1.07	0.15	3.48
KD33062a	82.0	82.5	1	4.96	1.96	0.05	5.10	19.14	0.87	1.18	-0.02	2.63
			2	4.78	1.85	0.04	4.76	16.92	0.93	1.17	0.00	2.51
			Avg.	4.87	1.91	0.04	4.93	18.03	0.90	1.18	-0.01	2.57
KD33062a	88.0	88.5	1	5.07	2.12	0.05	4.32	17.88	1.06	1.20	0.23	2.76
			2	4.87	2.10	0.06	4.45	18.23	0.80	1.13	0.00	2.60
			Avg.	4.97	2.11	0.05	4.38	18.06	0.93	1.16	0.12	2.68
KD33264	75.0	77.0	1	5.83	1.92	0.05	5.30	19.50	1.19	1.38	0.38	2.98
			2	5.17	1.82	0.05	4.90	17.70	0.92	1.22	-0.02	2.82
			Avg.	5.50	1.87	0.05	5.10	18.60	1.05	1.29	0.18	2.90
KD33264	89.0	90.25	1	5.22	1.96	0.06	5.04	19.88	1.20	1.28	0.39	2.48
			2	4.92	1.92	0.06	5.11	18.94	0.84	1.19	-0.01	2.28
			Avg.	5.07	1.94	0.06	5.07	19.41	1.02	1.23	0.19	2.38
KD33264	94.75	95.75	1	5.99	1.82	0.04	3.35	12.58	1.31	1.53	0.38	3.98
			2	6.05	2.02	0.05	3.67	13.60	1.07	1.65	-0.02	3.75
			Avg.	6.02	1.92	0.05	3.51	13.09	1.19	1.59	0.18	3.87
KD33262	45.2	46.2	1	4.62	2.00	0.05	6.56	21.78	0.86	1.10	0.45	1.75
			2	4.38	2.24	0.06	5.86	21.17	0.85	1.10	0.07	1.57
			Avg.	4.50	2.12	0.05	6.21	21.48	0.85	1.10	0.26	1.66
KD33262	52.75	53.75	1	5.56	1.98	0.04	4.93	17.65	51.08*	2.04	0.45	7.10
			2	5.52	1.94	0.04	4.21	16.37	0.98	1.39	0.03	4.66
			Avg.	5.54	1.96	0.04	4.57	17.01	0.98	1.72	0.24	5.88
KD33262	54.5	55.75	1	5.70	1.72	0.04	6.63	22.39	1.39	1.25	0.43	4.72
			2	4.52	1.82	0.05	5.66	20.92	0.78	1.11	0.04	4.28
			Avg.	5.11	1.77	0.04	6.14	21.66	1.09	1.18	0.24	4.50
Average standard deviation				0.20	0.08	0.00	0.27	0.75	0.15	0.08	0.21	0.23

* Not used.

2. Procedure for ferrous iron determination

Sediment samples were crushed to $<125\mu\text{m}$ (120 mesh). Approximately 0.4 g of each sample was weighed out on a calibrated analytical balance, and the weight was recorded to the nearest 0.1 mg. Each sample was transferred to a 50 ml Teflon beaker, and 10 ml of 1:1 H_2SO_4 (vol:vol) was added. The samples were placed on a hot plate at $\sim 90^\circ\text{C}$. After heating for 5 minutes, 10 ml of HF was added, and the samples were transferred to a second hot plate and taken to boiling. After 10 minutes, each sample was removed from the hot plate and placed, beaker and all, into a 500 ml beaker containing 200 ml deionized water; 15 ml 1:2 H_2SO_4 (vol:vol); 5 ml concentrated H_3PO_4 ; 25 ml saturated boric acid solution; and 6 drops of 0.2 % sodium diphenylamine sulfonate indicator solution. This solution was then titrated to a purple end-point with potassium dichromate solution (2.73 g/L), using a 50 ml burette read to the nearest 0.01 ml. The FeO content of the sample was calculated from the volume of titrant— one ml of dichromate solution is equal to 0.004 g FeO in the sample. Duplicates were run to evaluate precision and reproducibility—results are presented in Table A-2.

Table A-2. Results of duplicate analyses, ferrous iron.

Borehole #	Interval sampled, ft		FeO, %			Standard Deviation
	begin	end	Rep. 1	Rep. 2	Average	
KD33255	58.5	59.5	0.79	0.90	0.84	0.07
KD33262	55.8	57.1	0.49	0.59	0.54	0.07
KD33062a	58.0	58.5	0.90	1.09	0.99	0.13
KD33062a	100.0	100.5	1.18	0.89	1.04	0.20
KD33264	94.75	95.75	0.80	0.89	0.84	0.07
Average Standard Deviation						0.11

3. Procedure for total organic carbon determination

The carbon content of the sediment samples was determined using a UIC Inc. carbon coulometer with a furnace front-end. Sediment samples were crushed to $<125\mu\text{m}$ (120 mesh). Approximately 0.1 g of each sample was weighed out on a calibrated analytical balance, and the weight was recorded to the nearest 0.1 mg. Samples were quantitatively transferred to the quartz glass ladle used for introducing samples to the coulometer furnace. To remove inorganic carbon, 500 μl of concentrated HCl was added, in 100 μl increments, to the ladle, allowing carbonate digestion to cease before adding each increment. The ladle was then heated with a heat gun to promote complete reaction and to drive off excess acid. Care was taken not to scorch the sample, which could result in loss of organic carbon—if the sample turned black, it was discarded, and the process repeated. Once the sample was dry, it was introduced into the coulometer furnace at 900 C, and the CO_2 generated by oxidation of organic materials was quantified by the carbon coulometer. Blanks and synthetic standards were run periodically to monitor operating conditions, accuracy, and precision. Duplicate samples were analyzed to evaluate reproducibility—results are summarized in Table A-3.

Table A-3. Results of duplicate analyses, total organic carbon.

Borehole #	Interval sampled, ft		% TOC			Standard Deviation
	begin	end	Rep. 1	Rep. 2	Average	
KD33255	31.00	32.00	0.24	0.46	0.35	0.15
KD33255	83.25	84.00	0.36	0.38	0.37	0.01
KD33255	87.50	89.00	0.39	0.32	0.36	0.05
KD33262	45.20	46.20	0.33	0.32	0.33	0.01
KD33262	66.40	67.40	0.35	0.34	0.35	0.01
KD33264	48.00	49.50	0.24	0.24	0.24	0.00
KD33264	94.75	95.75	0.72	0.73	0.73	0.01
KD33062A	28.50	29.00	0.29	0.32	0.31	0.02
KD33062A	55.00	55.50	0.44	0.44	0.44	0.00
KD33062A	100.00	100.50	0.43	0.42	0.43	0.01
Average Standard Deviation						0.03

4. Clay mineral separation and preparation of oriented clay mounts for X-ray diffraction analysis

The clay minerals present in the aquifer sediment samples were identified by X-ray diffraction of oriented air-dried and glycolated clay mounts, using a Bruker D-8 Advance X-ray diffractometer (XRD) with a Kevex solid state X-ray detector.

The clay-sized ($<2 \mu\text{m}$) particle fraction was separated from the bulk sample using standard settling techniques. First, five grams of crushed sample was treated for one hour with 100 ml of 1.0 M sodium acetate (adjusted to pH 5 with acetic acid) to remove the carbonates. The sample was then centrifuged and rinsed repeatedly with 200 ml deionized water, until the solution remained milky after centrifugation. At this point, 50 mg of dispersant (sodium pyrophosphate) was added, and the sample was mixed for 15 minutes on an orbital mixer. It was then centrifuged for 15 minutes at 400 rpm (distance from center of rotation to solution midline = 13.0 cm), and the supernatant decanted off and saved. The procedure was repeated, and the supernatants, containing the clay size fraction, were combined.

Oriented clay X-ray mounts were made using the Millipore filter transfer method. Approximately 50 ml of the centrifuge supernatants was vacuum filtered through a $0.2 \mu\text{m}$ nylon filter, and the resulting clay filter cake was rinsed with several ml of 0.4 M $\text{Mg}(\text{NO}_3)_2$ to make the clays homoionic (to saturate the ion exchange positions in the smectites), and then rinsed with a few ml of deionized water to remove excess salts. This filter cake was then transferred to the XRD sample holder and the sample was allowed to dry. An X-ray diffraction pattern from 2° to $70^\circ 2\theta$ was collected.

After the air-dried samples were analyzed, they were solvated with ethylene glycol. The samples were placed in a dessicator with ethylene glycol in the bottom, and heated overnight at 60°C . The samples were then stored in a sealed container over an ethylene glycol bath until re-analysis by XRD.

5. Selective extraction procedure

The selective extractions were performed on two grams of uncrushed sample. Each sample was weighed out on an analytical balance and the weight recorded to four decimal places. The samples were quantitatively transferred to a 50 ml Oak Ridge style screw cap centrifuge tube.

In step 1, the exchangeable cation extraction, 40 ml of 0.4 M $\text{Mg}(\text{NO}_3)_2$ was added to the tube, and the samples were placed on hematology mixers for one hour. After one hour, the samples were centrifuged, and the supernatant decanted off and retained. Then, 20 ml of deionized water was added, and the sample was mixed for an additional 15 minutes. It was then re-centrifuged, and the supernatant decanted off and added to the previous fraction. The combined supernatants were acidified to 2% HNO_3 , brought to volume in a 100 ml volumetric flask, and saved for ICP-MS analysis.

In step 2, the exchangeable anion extraction, 40 ml of 0.1 M Na_2SO_4 was added to each sample and the samples were mixed on a hematology mixer for one hour and centrifuged. The supernatant was decanted off and retained. The sample was washed for 15 minutes with 20 ml deionized water, re-centrifuged, and the supernatant combined. The solution was acidified to 2% HNO_3 , brought to 100 ml final volume, and saved for ICM-MS analysis.

In step 3, carbonate minerals were removed. The samples were transferred quantitatively to 250 ml polyethylene centrifuge bottles, and 40 ml of 1.0 M sodium acetate, adjusted to pH 5 using acetic acid, was added. The samples were placed on an orbital platform mixer, and agitated, with the tops off, for four hours. The samples were centrifuged, and the supernatant retained. Because of the amount of carbonate present in the sediment, and because dolomite is only slowly attacked, carbonate remained in the sample at this point, and the procedure was repeated, allowing the samples to digest overnight. Finally, the sample was washed with 20 ml deionized water for 20 minutes, re-centrifuged, and the supernatant was collected. Initially, all three supernatants were combined, and the volume brought to 100 ml. Later, because of concerns about dissolution of iron oxides, the first aliquot was kept separate, brought to 50 ml total volume, and retained for ICP-MS analysis. The second aliquot and the rinse water were combined, brought to a volume of 100 ml, and retained for analysis.

In step 4, amorphous iron, manganese and aluminum oxides were extracted from the sample. In this step, 100 ml of 0.1 M oxalic acid/0.175 M ammonium oxalate was added to each sample, and the samples were agitated on an orbital platform mixer in the dark for four hours. The samples were then centrifuged and the supernatant decanted off. The sample was rinsed with 30 ml deionized water for 15 minutes, re-centrifuged, and the supernatants combined. The solution was brought to 200 ml total volume, and an aliquot saved for ICP-MS analysis.

In step 5, hydrogen peroxide was used to oxidize organic material in the samples. The samples were transferred to a hot water bath at 85° C, and 15 ml 0.02 M HNO_3 and 25 ml 30% H_2O_2 were added. The samples were heated for two hours, an additional 25 ml H_2O_2 was added, and the samples were heated for an additional three hours. Then, 40 ml of 1.0 M ammonium acetate adjusted to pH 2 with nitric acid was added, and the samples were transferred to an orbital platform mixer and agitated for 30 minutes. The sample was rinsed with 30 ml deionized water for 15 minutes, re-centrifuged, and the supernatants combined, brought to a volume of 100 ml, and retained for ICP-MS analysis.

In step 6, the crystalline Fe(III) oxides/hydroxides were removed from the sample using dithionite. Samples were placed in a hot water bath at 85 °C, and 100 ml of 0.3 M trisodium citrate/0.2 M sodium bicarbonate was added. After allowing the sample to reach temperature, 2.0 g of sodium dithionite was added, and the sample was stirred frequently by hand for ½ hour. The samples were then centrifuged, and the supernatant decanted off and retained. The extraction was repeated, and the supernatants combined. The sample was then rinsed with 30 ml of deionized water, and brought to a volume of 250 ml, an aliquot of which was retained for ICP-MS analysis.

In step 7, the sample was placed in a 95° C water bath, and 50 ml of 8 M HNO₃ was added. The sample bottle was covered with a watch glass and heated for 15 minutes. The sample was removed and allowed to cool, and an additional 5 ml conc. HNO₃ was added. The sample was placed back in the hot water bath and refluxed for an additional 30 minutes. The samples continued to generate brown fumes, so an additional 5 ml concentrated HNO₃ was added. The sample was heated for two hours, centrifuged, and the supernatant collected. The sample was rinsed for 15 minutes with 15 ml deionized water, and centrifuged again. The supernatants were combined in a Teflon beaker and brought to dryness. The sample was then brought to volume in 25 ml 1M HCl and retained for ICP-MS analysis.

In step 8, the residual solids were taken to dryness, crushed finely with a mortar and pestle, and weighed. Then, a 0.2 g aliquot was digested using the whole-rock digestion procedure described in Section 1 above. The sample was taken up in 25 ml 1M HCl, and retained for ICP-MS analysis.

Most samples were run in duplicate to assess the precision and reproducibility of the method. These data are presented in the main body of this report, and in Appendix B.

Appendix B. Major element data for sequential extractions

The amount of uranium released from the sediments samples during each step of the sequential extraction procedure is given in the main body of this report. The amount of each major element released in each step is tabulated here. Data are not included for Mg and Na, because in the first and second steps of the extraction procedure, respectively, the samples were contacted with solutions containing high concentrations of these elements. Uranium is included for completeness.

Table B-1. The results of sequential leaching experiments on sediment samples KD33262 45.2'–46.2' (uncontaminated) and KD33262 52.75'–53.75' (contaminated).

Sieve Size Fraction	Targeted uranium fraction	Uncontaminated (45.2' – 46.2')					
		Al ₂ O ₃ , %	Fe ₂ O ₃ , %	MnO, %	CaO, %	K ₂ O, %	U, ppm
Pan (<200 mesh)	Cation exchangeable	—	—	—	0.226	0.005	0.015
	Anion exchangeable	—	—	—	—	—	0.004
	Carbonate minerals	0.078	0.154	0.045	18.369	0.013	0.239
	Amorphous oxides	0.062	0.601	0.001	0.005	0.002	0.403
	Organics	0.010	0.035	0.002	2.326	0.005	0.189
	Crystalline Oxides	0.061	1.168	0.009	7.892	0.325	0.200
	Strong acid leachable	0.538	0.514	0.006	3.964	0.093	0.375
	Residual	2.202	0.361	0.004	0.386	0.785	0.879
	Totals:	2.950	2.833	0.068	33.167	1.227	2.303
40-60 mesh	Cation exchangeable	—	—	—	0.148	0.003	0.008
	Anion exchangeable	—	—	—	—	—	0.037
	Carbonate minerals	0.012	0.155	0.025	16.608	0.012	0.299
	Amorphous oxides	0.023	0.201	0.001	0.009	0.001	0.082
	Organics	0.019	0.040	0.001	0.555	0.004	0.122
	Crystalline Oxides	0.070	0.546	0.003	2.477	0.326	0.077
	Strong acid leachable	0.372	0.382	0.004	0.290	0.052	0.274
	Residual	4.318	0.825	0.018	0.703	0.943	0.640
	Totals:	4.814	2.149	0.051	20.789	1.342	1.542
10-20 mesh	Cation exchangeable	—	—	—	0.106	0.002	0.003
	Anion exchangeable	—	—	—	—	—	0.009
	Carbonate minerals	0.020	0.221	0.034	19.897	0.009	0.235
	Amorphous oxides	0.018	0.121	0.001	0.006	0.002	0.078
	Organics	0.010	0.046	0.001	2.297	0.011	0.099
	Crystalline Oxides	0.027	0.414	0.002	2.374	0.236	0.087
	Strong acid leachable	0.521	0.682	0.008	1.710	0.049	0.242
	Residual	3.505	0.591	0.007	0.668	0.808	0.459
	Totals:	4.101	2.075	0.054	27.057	1.116	1.212
Whole rock	Cation exchangeable	—	—	—	0.152	0.003	0.010
	Anion exchangeable	—	—	—	—	—	0.011
	Carbonate minerals	0.014	0.197	0.032	18.683	0.013	0.303
	Amorphous oxides	0.020	0.180	0.001	0.007	0.002	0.117
	Organics	0.013	0.039	0.001	1.167	0.007	0.142
	Crystalline Oxides	0.032	0.517	0.002	2.535	0.220	0.118
	Strong acid leachable	0.488	0.517	0.006	1.292	0.072	0.400
	Residual	3.561	0.564	0.008	0.384	0.882	0.705
	Totals:	4.127	2.014	0.051	24.219	1.199	1.807

Table B-1. Continued.

Sieve Size Fraction	Targeted uranium fraction	Contaminated (52.75' - 53.75')					
		Al ₂ O ₃ , %	Fe ₂ O ₃ *, %	MnO, %	CaO, %	K ₂ O, %	U, ppm
Pan (<200 mesh)	Cation exchangeable	—	—	—	0.262	0.006	2.766
	Anion exchangeable	—	—	—	—	—	0.515
	Carbonate minerals	0.019	0.192	0.035	16.226	0.018	5.502
	Amorphous oxides	0.242	1.745	0.006	0.091	0.008	0.846
	Organics	0.041	0.072	0.001	0.495	0.007	0.338
	Crystalline Oxides	0.032	0.352	0.002	3.952	0.214	0.451
	Strong acid leachable	0.794	0.572	0.005	0.528	0.153	0.768
	Residual	2.994	0.477	0.003	0.229	1.066	1.302
	Totals:	4.122	3.411	0.053	21.782	1.473	12.489
100-200 mesh	Cation exchangeable	—	—	—	0.212	0.005	1.463
	Anion exchangeable	—	—	—	—	—	0.323
	Carbonate minerals	0.014	0.185	0.028	14.381	0.016	3.360
	Amorphous oxides	0.125	1.049	0.003	0.047	0.002	0.606
	Organics	0.016	0.036	0.001	0.547	0.005	0.410
	Crystalline Oxides	0.025	0.373	0.003	2.984	0.227	0.348
	Strong acid leachable	0.774	0.660	0.007	1.103	0.147	0.886
	Residual	3.233	1.835	0.026	0.663	1.060	0.966
	Totals:	4.188	4.139	0.067	19.937	1.461	8.362
60-100 mesh	Cation exchangeable	—	—	—	0.158	0.003	0.660
	Anion exchangeable	—	—	—	—	—	0.186
	Carbonate minerals	0.011	0.122	0.017	10.765	0.011	1.930
	Amorphous oxides	0.063	0.477	0.001	0.048	0.001	0.271
	Organics	0.017	0.025	0.001	0.405	0.005	0.191
	Crystalline Oxides	0.022	0.232	0.002	1.463	0.235	0.159
	Strong acid leachable	0.477	0.382	0.005	0.793	0.095	0.570
	Residual	4.934	1.048	0.022	0.827	1.176	0.637
	Totals:	5.523	2.286	0.047	14.459	1.526	4.604
40-60 mesh	Cation exchangeable	—	—	—	0.113	0.002	0.391
	Anion exchangeable	—	—	—	—	—	0.254
	Carbonate minerals	0.008	0.113	0.015	9.716	0.012	1.585
	Amorphous oxides	0.048	0.332	0.001	0.051	0.001	0.326
	Organics	0.022	0.042	0.001	0.451	0.004	0.257
	Crystalline Oxides	0.019	0.211	0.001	1.110	0.230	0.125
	Strong acid leachable	0.352	0.291	0.003	0.283	0.062	0.277
	Residual	5.189	0.421	0.008	0.630	1.281	0.628
	Totals:	5.638	1.410	0.029	12.354	1.592	3.842

Table B-1. Continued.

Sieve Size Fraction	Targeted uranium fraction	Contaminated (52.75' - 53.75')					
		Al ₂ O ₃ , %	Fe ₂ O ₃ *, %	MnO, %	CaO, %	K ₂ O, %	U, ppm
20-40 mesh	Cation exchangeable	—	—	—	0.116	0.002	0.302
	Anion exchangeable	—	—	—	—	—	0.118
	Carbonate minerals	0.010	0.701	0.028	13.702	0.012	1.790
	Amorphous oxides	0.063	0.365	0.001	0.049	0.001	0.480
	Organics	0.028	0.037	0.001	0.423	0.005	0.256
	Crystalline Oxides	0.032	0.266	0.002	2.062	0.226	0.191
	Strong acid leachable	0.419	0.397	0.005	0.818	0.074	0.478
	Residual	3.266	0.348	0.004	0.450	0.929	0.658
	Totals:	3.818	2.114	0.038	17.621	1.249	4.271
10-20 mesh	Cation exchangeable	—	—	—	0.085	0.002	0.188
	Anion exchangeable	—	—	—	—	—	0.072
	Carbonate minerals	0.005	0.082	0.014	16.083	0.000	1.790
	Amorphous oxides	0.052	0.265	0.002	0.044	0.001	0.507
	Organics	0.018	0.035	0.001	0.520	0.005	0.185
	Crystalline Oxides	0.022	0.297	0.002	2.919	0.223	0.281
	Strong acid leachable	0.506	0.679	0.009	3.636	0.064	0.465
	Residual	3.234	0.405	0.005	0.315	0.835	1.238
	Totals:	3.836	1.763	0.032	23.601	1.129	4.726
4-10 mesh	Cation exchangeable	—	—	—	0.047	0.001	0.076
	Anion exchangeable	—	—	—	—	—	0.031
	Carbonate minerals	0.010	0.232	0.034	19.956	0.012	1.189
	Amorphous oxides	0.024	0.115	0.001	0.042	0.000	0.218
	Organics	0.017	0.043	0.001	0.629	0.004	0.120
	Crystalline Oxides	0.015	0.197	0.002	2.248	0.222	0.155
	Strong acid leachable	0.362	0.543	0.009	4.802	0.053	0.324
	Residual	2.357	0.434	0.004	0.359	0.593	0.362
	Totals:	2.785	1.564	0.050	28.082	0.885	2.474
Whole rock	Cation exchangeable	—	—	—	0.159	0.003	0.525
	Anion exchangeable	—	—	—	—	—	0.158
	Carbonate minerals	0.009	0.174	0.022	13.552	0.011	1.879
	Amorphous oxides	0.067	0.413	0.003	0.049	0.001	0.330
	Organics	0.032	0.042	0.001	0.395	0.005	0.218
	Crystalline Oxides	0.333	0.230	0.003	1.991	0.212	0.446
	Strong acid leachable	0.359	0.332	0.004	2.180	0.074	0.272
	Residual	4.300	0.557	0.009	0.499	1.114	0.630
	Totals:	5.100	1.748	0.041	18.824	1.420	4.458

Table B-2. The results of sequential extraction experiments, samples from borehole KD33062A, KD33255, and KD33264.

Sieve Size Fraction	Targeted uranium fraction	KD33062A (64.5' - 65.0')					
		Al ₂ O ₃ , %	Fe ₂ O ₃ , %	MnO, %	CaO, %	K ₂ O, %	U, ppm
Pan (<200 mesh) Sample A	Cation exchangeable	—	—	—	0.286	0.007	1.51
	Anion exchangeable	—	—	—	0.069	0.004	0.25
	Carbonate minerals (1)	0.010	0.142	0.0523	12.506	0.006	4.05
	Carbonate minerals (2)	0.011	0.111	0.0349	9.013	0.008	0.93
	Amorphous oxides	0.059	0.544	0.1003	0.039	0.001	0.88
	Organics	0.014	0.054	0.0051	1.111	0.008	0.12
	Crystalline Oxides	0.082	1.523	0.0252	2.498	0.172	0.30
	Strong acid leachable	0.531	0.468	0.0048	0.056	0.087	0.35
	Residual	3.039	0.333	0.0040	0.298	0.891	0.84
	Totals:	3.745	3.177	0.227	25.874	1.183	9.23
Pan (<200 mesh) Sample B	Cation exchangeable	—	—	—	0.300	0.008	1.43
	Anion exchangeable	—	—	—	0.088	0.019	0.26
	Carbonate minerals (1)	0.009	0.137	0.0516	12.492	0.006	4.34
	Carbonate minerals (2)	0.011	0.110	0.0340	9.003	0.008	0.83
	Amorphous oxides	0.062	0.568	0.1021	0.053	0.000	0.90
	Organics	0.013	0.063	0.0055	1.242	0.008	0.31
	Crystalline Oxides	0.058	1.145	0.0190	1.919	0.153	0.25
	Strong acid leachable	0.651	0.553	0.0051	0.072	0.099	0.36
	Residual	2.152	0.350	0.0064	0.445	0.598	0.39
	Totals:	2.956	2.927	0.224	25.614	0.899	9.07
Whole rock Sample A	Cation exchangeable	—	—	—	0.162	0.003	0.29
	Anion exchangeable	—	—	—	0.091	0.004	0.10
	Carbonate minerals (1)	0.003	0.133	0.0429	10.960	0.005	0.90
	Carbonate minerals (2)	0.004	0.121	0.0293	9.145	0.007	0.37
	Amorphous oxides	0.014	0.122	0.0018	0.023	-0.001	0.23
	Organics	0.011	0.037	0.0050	1.382	0.008	0.27
	Crystalline Oxides	0.027	0.430	0.0014	0.897	-0.301	0.23
	Strong acid leachable	0.347	0.355	0.0064	2.216	0.053	0.27
	Residual	3.601	0.428	0.0049	0.316	1.124	1.08
	Totals:	4.006	1.625	0.092	25.193	0.903	3.74
Whole rock Sample B	Cation exchangeable	—	—	—	0.137	0.003	0.19
	Anion exchangeable	—	—	—	0.076	0.003	0.08
	Carbonate minerals (1)	0.003	0.107	0.0262	9.833	0.005	0.84
	Carbonate minerals (2)	0.004	0.099	0.0171	9.066	0.007	0.42
	Amorphous oxides	0.010	0.102	0.0022	0.028	0.000	0.21
	Organics	0.005	0.040	0.0037	2.169	0.008	0.14
	Crystalline Oxides	0.025	0.430	0.0027	1.883	0.165	0.17
	Strong acid leachable	0.320	0.403	0.0074	4.516	0.046	0.21
	Residual	3.623	0.573	0.0083	0.574	1.105	0.55
	Totals:	3.990	1.753	0.068	28.281	1.342	2.79

Table B-2. Cont.

Sieve Size Fraction	Targeted uranium fraction	KD33255 (73.0' - 74.5')					
		Al ₂ O ₃ , %	Fe ₂ O ₃ *, %	MnO, %	CaO, %	K ₂ O, %	U, ppm
Pan (<200 mesh) Sample A	Cation exchangeable	—	—	—	0.291	0.008	2.08
	Anion exchangeable	—	—	—	0.058	0.005	0.37
	Carbonate minerals (1)	0.010	0.114	0.050	10.553	0.006	3.25
	Carbonate minerals (2)	0.012	0.121	0.038	9.015	0.007	0.85
	Amorphous oxides	0.072	1.125	0.009	0.026	0.003	0.82
	Organics	0.014	0.049	0.003	1.111	0.008	0.28
	Crystalline Oxides	0.059	1.360	0.009	2.691	0.161	0.26
	Strong acid leachable	0.595	0.522	0.005	0.178	0.097	0.58
	Residual	2.903	0.327	0.004	0.247	0.849	0.90
	Totals:	3.664	3.617	0.118	24.170	1.144	9.39
Pan (<200 mesh) Sample B	Cation exchangeable	—	—	—	0.285	0.007	2.07
	Anion exchangeable	—	—	—	0.056	0.005	0.38
	Carbonate minerals (1)	0.011	0.110	0.051	10.684	0.006	3.95
	Carbonate minerals (2)	0.012	0.123	0.038	8.938	0.007	0.80
	Amorphous oxides	0.059	0.935	0.008	0.032	0.000	0.80
	Organics	0.013	0.046	0.003	1.173	0.008	0.31
	Crystalline Oxides	0.061	1.466	0.010	2.863	0.158	0.20
	Strong acid leachable	0.578	0.525	0.005	0.156	0.099	0.59
	Residual	2.696	0.313	0.004	0.234	0.846	0.75
	Totals:	3.429	3.518	0.118	24.422	1.135	9.84
Whole rock Sample A	Cation exchangeable	—	—	—	0.134	0.003	0.23
	Anion exchangeable	—	—	—	0.074	0.004	0.10
	Carbonate minerals (1)	0.006	0.201	0.048	16.906	0.009	1.58
	Carbonate minerals (2)	0.004	0.086	0.015	6.546	0.007	0.36
	Amorphous oxides	0.016	0.167	0.006	0.050	-0.001	0.20
	Organics	0.012	0.101	0.001	0.636	0.007	0.12
	Crystalline Oxides	0.027	0.425	0.003	1.764	0.150	0.06
	Strong acid leachable	0.389	0.489	0.006	2.812	0.059	0.22
	Residual	3.235	0.521	0.006	0.434	0.705	0.51
	Totals:	3.690	1.991	0.085	29.355	0.944	3.41
Whole rock Sample B	Cation exchangeable	—	—	—	0.157	0.004	0.29
	Anion exchangeable	—	—	—	0.073	0.004	0.11
	Carbonate minerals (1)	0.007	0.149	0.034	12.647	0.009	1.84
	Carbonate minerals (2)	0.006	0.084	0.011	6.694	0.007	0.61
	Amorphous oxides	0.028	0.313	0.006	0.057	0.015	0.25
	Organics	0.010	0.072	0.001	0.665	0.006	0.26
	Crystalline Oxides	0.032	0.663	0.003	1.904	0.157	0.214
	Strong acid leachable	0.640	0.482	0.005	1.658	0.057	0.312
	Residual	1.826	0.255	0.004	0.247	0.598	0.364
	Totals:	2.548	2.017	0.063	24.102	0.857	4.25

Table B-2. Cont.

Sieve Size Fraction	Targeted uranium fraction	KD33264 (79.5' - 83.25')					
		Al ₂ O ₃ , %	Fe ₂ O ₃ , %	MnO, %	CaO, %	K ₂ O, %	U, ppm
Pan (<200 mesh) Sample A	Cation exchangeable	—	—	—	0.346	0.011	0.74
	Anion exchangeable	—	—	—	0.075	0.004	0.41
	Carbonate minerals (1)	0.004	0.065	0.021	5.088	0.004	1.50
	Carbonate minerals (2)	0.009	0.097	0.008	5.946	0.007	0.57
	Amorphous oxides	0.051	0.497	0.003	0.059	0.000	0.95
	Organics	0.009	0.118	0.002	1.046	0.008	0.43
	Crystalline Oxides	0.059	1.427	0.005	1.795	0.191	0.39
	Strong acid leachable	0.756	0.674	0.006	0.174	0.129	0.93
	Residual	2.802	0.457	0.003	0.232	1.053	1.32
	Totals:	3.690	3.335	0.049	14.761	1.408	7.24
Pan (<200 mesh) Sample B	Cation exchangeable	—	—	—	0.338	0.012	0.88
	Anion exchangeable	—	—	—	0.087	0.005	0.35
	Carbonate minerals (1)	0.005	0.068	0.022	5.485	0.005	1.54
	Carbonate minerals (2)	0.009	0.097	0.009	5.870	0.007	0.64
	Amorphous oxides	0.050	0.484	0.003	0.062	0.001	1.22
	Organics	0.016	0.073	0.001	0.355	0.009	0.23
	Crystalline Oxides	0.047	1.522	0.006	1.728	0.169	0.28
	Strong acid leachable	0.694	0.636	0.006	0.128	0.127	0.84
	Residual	4.176	0.470	0.005	0.385	1.224	1.70
	Totals:	4.996	3.351	0.050	14.438	1.558	7.70
Whole rock Sample A	Cation exchangeable	—	—	—	0.133	0.005	0.13
	Anion exchangeable	—	—	—	0.069	0.003	0.09
	Carbonate minerals (1)	0.002	0.044	0.012	3.658	0.003	0.41
	Carbonate minerals (2)	0.003	0.049	0.007	3.463	0.005	0.24
	Amorphous oxides	0.019	0.134	0.001	0.065	0.001	0.23
	Organics	0.009	0.105	0.003	0.836	0.007	0.36
	Crystalline Oxides	0.044	0.477	0.004	1.477	0.176	0.23
	Strong acid leachable	0.353	0.388	0.009	3.031	0.078	0.53
	Residual	4.149	0.609	0.008	1.187	1.127	0.85
	Totals:	4.580	1.807	0.045	13.919	1.403	3.08
Whole rock Sample B	Cation exchangeable	—	—	—	0.147	0.006	0.16
	Anion exchangeable	—	—	—	0.067	0.003	0.07
	Carbonate minerals (1)	0.002	0.046	0.011	4.261	0.004	0.44
	Carbonate minerals (2)	0.004	0.062	0.007	4.555	0.006	0.27
	Amorphous oxides	0.017	0.124	0.001	0.062	0.000	0.23
	Organics	0.012	0.087	0.001	0.429	0.007	0.24
	Crystalline Oxides	0.045	0.389	0.003	1.598	0.142	0.26
	Strong acid leachable	0.394	0.504	0.010	3.004	0.072	0.54
	Residual	3.980	0.419	0.004	0.410	1.296	0.68
	Totals:	4.454	1.632	0.037	14.532	1.536	2.88

Table B-3. The results of sequential extraction experiments on 0.1 M carbonate leached samples of the pan (<200 mesh) fraction, sample KD33262 52.75'–53.75'.

Replicate #	Targeted uranium fraction	KD33262 52.75' – 53.75', pan (<200 mesh) fraction, 0.1 M carbonate treated					
		Al ₂ O ₃ , %	Fe ₂ O ₃ *, %	MnO, %	CaO, %	K ₂ O, %	U, ppm
Sample A	0.1 M carbonate soln.	—	0.019	—	0.029	0.007	5.57
	Cation exchangeable	—	—	—	0.257	0.007	0.18
	Anion exchangeable	—	—	—	—	—	0.10
	Carbonate minerals	0.033	0.294	0.038	18.078	0.008	2.94
	Amorphous oxides	0.135	1.355	0.002	0.134	0.003	0.71
	Organics	0.073	0.054	0.001	0.054	0.005	0.41
	Crystalline Oxides	0.039	0.649	0.002	0.699	0.255	0.00
	Strong acid leachable	0.533	0.462	0.004	0.025	0.118	0.58
	Residual	2.500	0.438	0.003	0.153	1.046	0.92
	Totals:	3.314	3.253	0.050	19.400	1.440	5.85
Sample B	0.1 M carbonate soln.	—	0.018	—	0.027	0.007	4.89
	Cation exchangeable	—	—	—	0.254	0.007	0.17
	Anion exchangeable	—	—	—	—	—	0.05
	Carbonate minerals	0.032	0.297	0.038	20.168	0.009	2.92
	Amorphous oxides	0.140	1.330	0.002	0.137	0.003	0.68
	Organics	0.067	0.052	0.001	0.076	0.005	0.36
	Crystalline Oxides	0.083	0.658	0.002	1.168	0.256	-0.02
	Strong acid leachable	0.590	0.476	0.005	0.030	0.128	0.77
	Residual	4.000	0.438	0.004	0.197	1.153	1.62
	Totals:	4.912	3.251	0.052	22.030	1.561	6.55